

HALF-YEAR REPORT
(Oct. 1978 - Mar. 1979)
HEAVY ION FUSION PROGRAM
LAWRENCE BERKELEY LABORATORY

NOTICE

This report was prepared as an account of work sponsored by the United States Government. Neither the United States nor the United States Department of Energy, nor any of their employees, nor any of their contractors, subcontractors, or their employees, make any warranty, express or implied, or assumes any legal liability or responsibility for the accuracy, completeness or usefulness of any information, apparatus, product or process disclosed, or represents that its use would not infringe privately owned rights.

CONTENTS

HIGHLIGHTS

PART I ACTIVITIES RELEVANT TO INDUCTION LINAC SYSTEMS

1.1 High-Current Cesium Ion Beam

- 1.1.1 Cesium Source
- 1.1.2 Spark Oven Tests
- 1.1.3 Large Cryo-pump

1.2 Systems Studies

- 1.2.1 "One Kilojoule" Test Bed Preliminary Conceptual Design
- 1.2.2 System Design and Cost Results (LIACEP)

1.3 Engineering Tests

- 1.3.1 Core Material Evaluation
- 1.3.2 Pulse Power Tests

PART II ACTIVITIES RELEVANT TO R.F. LINAC/STORAGE RINGS SYSTEMS

2.1 High-Current Xenon Beam Results

- 2.1.1 Xenon Ion Source
- 2.1.2 Acceleration of Xe^{+1} to 0.5 MV

2.2* r.f. Linac Systems

- 2.2.1* Wideröe r.f. Linac Design
- 2.2.2* Emittance Growth in r.f. Linac
- 2.2.3* Future Plans for High Energy Heavy Ion Facilities

2.3* Ion-Ion Cross-Section (Cs^{+1} , Cs^{+1}) Program

PART III THEORY

PART IV OTHER ACTIVITIES

- 4.1 The Cost of HIF Power
- 4.2 Completion of High-Bay Extension

PART V HEAVY ION FUSION NOTES: Reports Index (10/1/78-3/31/79)

PART VI APPENDICES:

- A. S. Abbott, et al, "Large-Aperture Contact-Ionized Cs⁺¹ Ion Source for an Induction Linac," LBL-8359, 1979 Particle Accelerator Conf., San Francisco, March 12-14, 1979.
- B. A. Faltens, et al, "Design/Cost Study of an Induction Linac for Heavy Ions for Pellet-Fusion," LBL-8357, Ibid.
- C. W. Chupp, et al, "Operation of a High Current Xenon Source," LBL-8859, Ibid.
- D. J.W. Staples, et al, "A Wideröe-Based Heavy Ion Preaccelerator for the Superhilac," LBL-8810, Ibid.
- E. J.W. Staples, R.A. Jameson, "Possible Lower Limit to Linac Emittance," LBL-8809, Ibid.
- F. C. Leeman, "Prospects for High Energy Heavy Ion Accelerators," LBL-8899, Ibid.
- G. L.J. Laslett, L. Smith, "Stability of Intense Transported Beams," LBL-8382, Ibid.
- H. D. Neuffer, "Longitudinal Motion in High Current Ion Beams--A Self-Consistent Phase Space Distribution with an Envelope Equation," LBL-8387, Ibid.

Heavy-Ion Fusion Half-Year Report
October 1978 - March 1979
Lawrence Berkeley Laboratory
University of California, Berkeley

HIGHLIGHTS

Among the more important results and activities reported in this Half-Year Report are:

- Commissioning, in January 1979, of a large-area Cs^{+1} ion source of 1.2 amperes at 500 kV. This source has a repetition rate of 1 per second and is on a scale suitable for an induction linac.
- Commissioning, in August 1978, of a small aperture, high-brightness Xe^{+1} source of 65 mA at 20 kV suitable for an rf linac.
- Acceleration, in January 1979, of the Xe^{+1} beam through a Cockcroft-Walton column to 500 kV and confirmation of satisfactory emittance and charge distribution.
- Presentation at the IEEE Particle Accelerator Conference, San Francisco, March 1979, of eight papers from this laboratory bearing on topics of interest to induction and rf linac drivers. (See Appendices A through H).
- Start-up of a (Cs^{+1} , Cs^{+1}) ion-ion cross-section measurement program.

PART I ACTIVITIES RELEVANT TO INDUCTION LINAC SYSTEMS

1.1 HIGH-CURRENT CESIUM ION BEAM

1.1.1 Cesium Source (C. Kim)

The large area (30 cm dia.) cesium ion source has been put into operation at the full design voltage, 500 kV, and design beam-current, 1.2 amps. The reproducibility of the space-charge-limited ion current and the voltage waveforms has been demonstrated at repetition rates up to 1 hertz. A detailed description of the source construction, operation and performance is given in Appendix A.

Recently, the beam profile and emittance have been studied. The beam profile measured with a radially scanning probe placed downstream of the cathode grid shows a fine structure near the grid apparently generated as a result of beam focusing by the grid (Fig. 1). The fine structure disappears as the probe is moved further downstream approximately 1.3 meters away from the grid, which implies an estimated normalized emittance of $2 \times 10^{-6} \pi$ rad-m. Other emittance measurements using slots agree with this number.

The beam diameter monitored at 1.7 m from the anode was found to be a strong function of the current if the beam is emission limited. The beam diameter is independent of the voltage when the current is space charge limited as predicted by theory. The space charge limited beam diameter at 1.7 m is about 8 cm, about a factor of three smaller than the beam diameter at the cathode grid. Figure 2 shows the beam profile monitored on the KBr scintillator for (a) a space charge limited beam and (b) an emission limited beam.

1.1.2 Cesium Spark Oven (J. Shiloh)

A pulsed cesium vapor oven utilizing a vacuum spark has been developed in order to replace the continuous supply of Cs vapor currently used.¹ The spark oven will provide a burst of neutral Cs atoms aimed at the hot plate such that $\sim 1\%$ of a monolayer of adsorbed Cesium atoms covers the surface. The Marx generator is fired ~ 10 ms after the spark source to allow time for the remaining vapor to leave the diode gap.

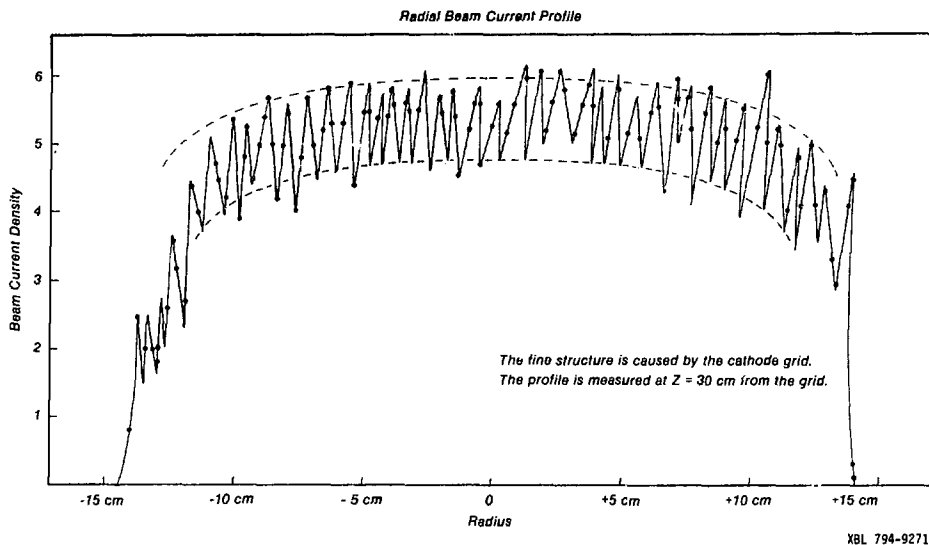


Fig. 1. Beam profile measured with a scanning probe showing the fine structure generated by the cathode grid.

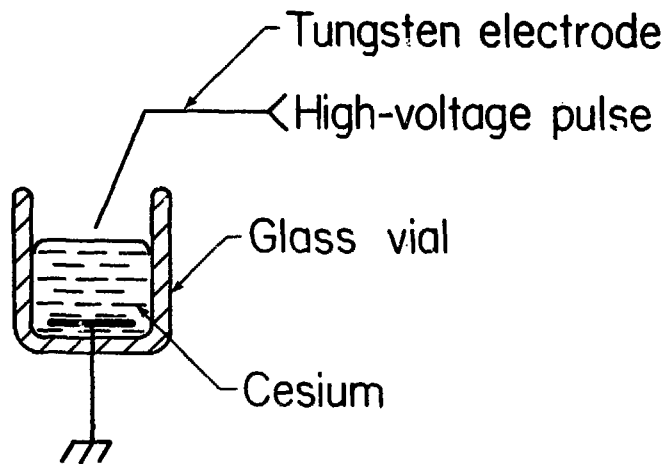


Fig. 2. Beam profile monitored on the KBr scintillator plate (a) for a space charge limited beam (350 kV, 800 mA, and (b) for an emission limited beam (350 kV, 400 mA). In both cases the beam is 10 μ sec long. The screw marks are 7.2 cm apart vertically.

Experiments with such a spark oven have been carried out on a 200 kV test stand. The spark oven consists of a 1 cm diameter glass vial filled with cesium, and two electrodes (Fig. 1), one in contact with the cesium metal and the other located a few millimeters above the cesium surface. A vacuum spark is initiated between the top electrode and the cesium by discharging a 4 μ F capacitor through the gap. The capacitor charging voltage can be varied in the range of 7-15 kV. The measured Cs^{+1} ion current as a function of the spark and the Marx voltages is shown in Fig. 2, for a hot plate temperature of 1080°C and a delay of 10 ms between the spark and the Marx voltage. At low spark voltages the ion current is emission limited, i.e., not enough Cs vapor reaches the hot plate. However, at a charging voltage of 15 kV the current is limited by the space charge of the beam. The highest current density exceeds 1 mA/cm² which is comparable to the current density required for the operation of the 500 kV, 1 amp system. In order to determine the hot plate coverage as a function of the delay between the spark and the Marx generator voltage, the system was operated in the emission limited mode (Marx voltage - 70 kV, spark charging voltage - 10 kV). The observed current for two temperatures is shown in Fig. 3. The Cs vapor burst lasts \sim 1 ms and 5-10 ms time delay is allowed for the rest of the Cs vapor to leave the diode gap. Such a delay, at an operating temperature of 1080°C is appropriate under normal operating conditions. The spark oven unit is scheduled to be installed on the 500 kV system in April 1979.

In addition to the Cs oven we are now studying the possibilities of using alumino-silicate sources to deliver the necessary Cs^{+1} ion current. Alumino-silicate ion sources are known to supply low currents ($< 1 \text{ mA/cm}^2$) under continuous low voltage operation. However, current densities of Cs^{+1} ions as high as 1 Amp/cm² have been achieved in pulsed operation.² The use of an alumino-silicate source may be extended in the future to include thallium.³

1. HIF Quarterly Report, Dec. 31, 1978 (HI-FAN-68).
2. A.N. Pargellis and M. Seidl, J. Appl. Phys. 49, 4933, 1978.
3. R.K. Feeney, et al., Rev. Sci. Instrum. 47, 964 (1976).



-5-

XBL 794-1267

Fig. 1. Cesium spark source--schematic

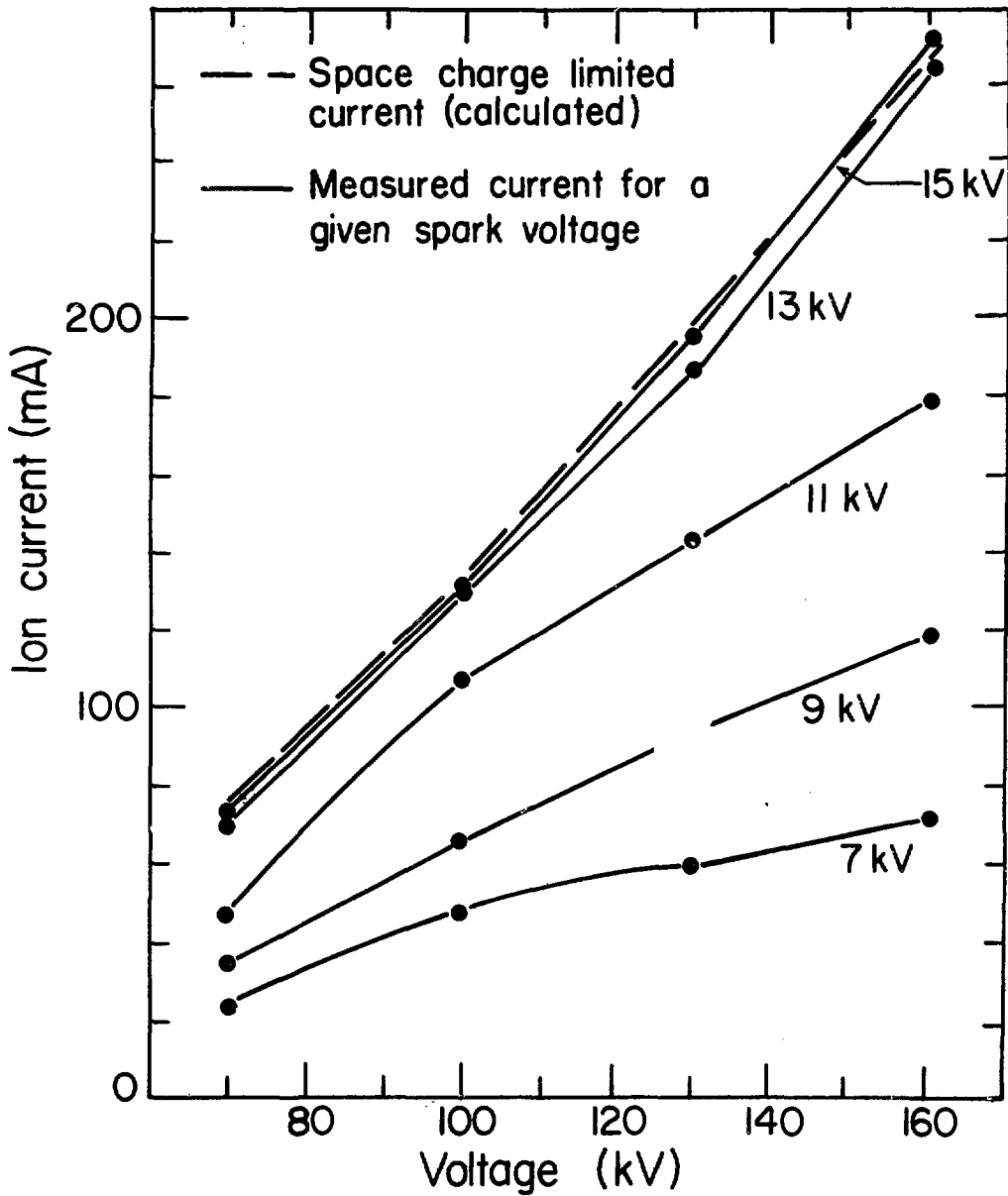


Fig. 2. Cs⁺ ion current as a function of the diode voltage for different charging voltages on the spark source.

XBL 794-1269

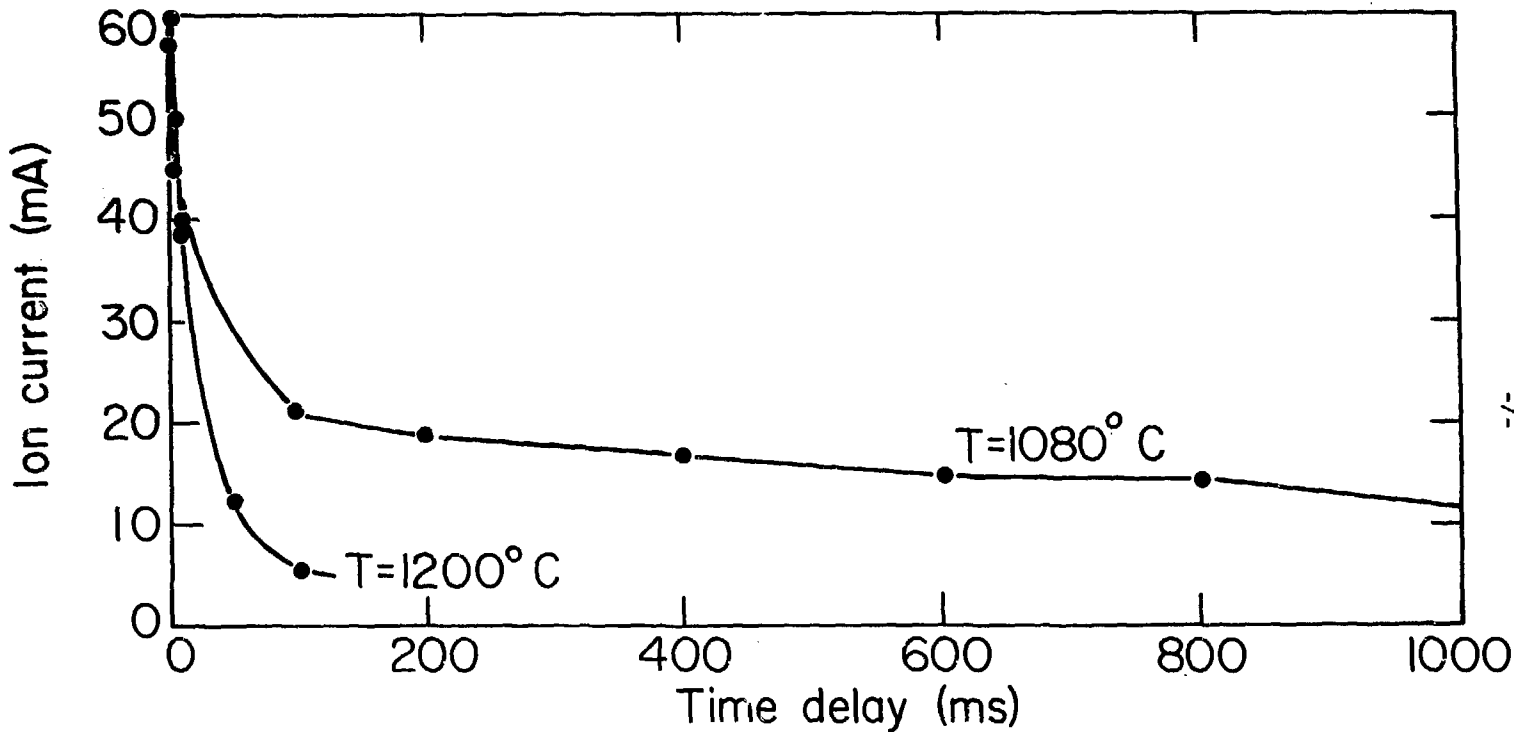


Fig. 3. Cs⁺ ion current as a function of the time delay between the spark and the Marx voltage.

XBL 794-1266

1.1.3 Large Cryopump (E. Hoyer)

For the 1 ampere Cesium ion source, better chamber vacuum has been desired to improve beam quality (by reducing ionization, charge exchange and charge stripping collisions) and to reduce high voltage insulator contamination. To improve the chamber vacuum, a cryocondensation pump, shown in Figs. 1 and 2, was designed, built and successfully operated. With the pump, an order of magnitude improvement in vacuum pressure was achieved bringing the chamber pressure down to the low 10^{-7} torr range.

The cryopump is of simple design and construction. Its three part design, shown in Fig. 3, consists of:

- 1) Innermost, a stainless steel vessel (for pool-boiling helium) and copper fins which provides a 4-5°K surface for pumping primarily N_2 , O_2 , CO, etc.
- 2) Surrounding the helium cooled surface is a LN cooled shield and large chevron, operating near 100°K, which pumps primarily water vapor and cesium. The large chevron assembly is a welded aluminum structure fabricated from commercially available angle and tubing.
- 3) Outermost, the water cooled chevron assembly, of similar construction to the LN cooled chevron, shields the LN cooled chevron from the iridium hot plate radiant energy.

Estimated cryopump pumping speeds in ℓ /sec are: 35,000 for water vapor, 12,000 for cesium vapor, and 12,000 for air. A N_2 pumping speed of 12,000 ℓ /sec was measured. The steady state liquid helium consumption is 0.8 ℓ /hr.

1.2 "ONE-KILOJOULE" INDUCTION LINAC TEST BED

1.2.1 Design Concept

A number of important technical questions would be answered and the operation of a significant number of accelerator components demonstrated by designing, building, and operating a 25 MeV Cs^{+1} linear induction accelerator. The present LBL experimental program is



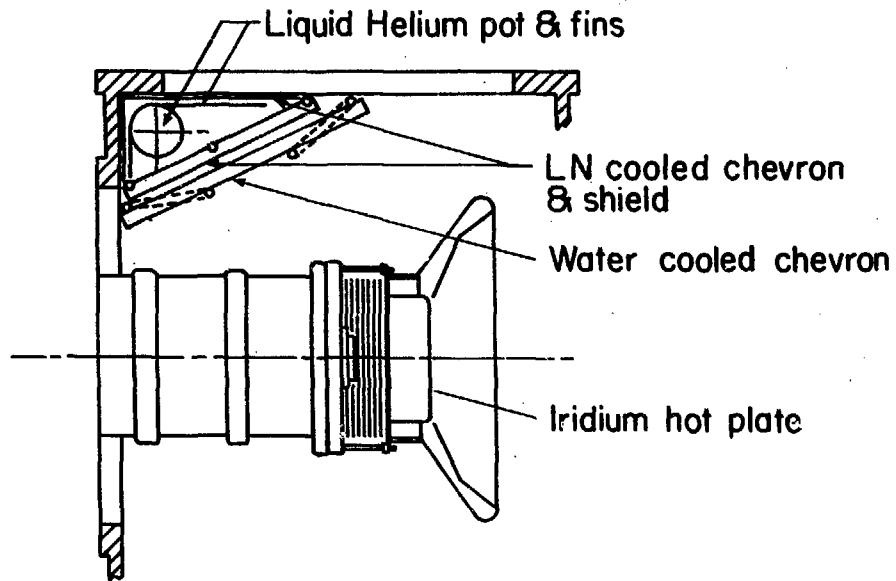
CBB-793-4050

Fig. 1. Cesium Ion Source Cryopump - Front view
showing water baffles



CBB-793-4048

Fig. 2. Cesium Ion Source Cryopump - Side View
showing LN shield



XBL 794-1263

Fig. 3. Ion Source Chamber Plan View.

developing a 2 MeV, 2 μC Cs^{+1} source, while a 1 MJ 100 TW test driver would require about 200 μC , therefore a 20 μC total charge is appropriate for an intermediate experiment. Such an accelerator requires approximately 87 magnets and 87 acceleration modules each of about 1 meter length, and would be sufficiently long to demonstrate transverse and longitudinal beam control. Previous HIDE conceptual designs have shown that the largest fractional energy tilt and the most stringent focusing requirements in a cost-optimized LIA occur at the low energy end of the machine. Therefore the intermediate experiment would address the most significant problems of HIDE; confirmation of the theoretical predictions would make the confidence level of HIDE very high.

In order to avoid mixing problems of beam control with problems associated with new technology, the design of the intermediate experiment will be based on a low field magnet system, existing and readily available core materials, and a low current injector. As the newer technology items become available they will be included in the design in a substitutional manner, perhaps operating below their capacity, in order to gain experience with them, but never in such a way that the operation of the accelerator is contingent on them. After or in parallel with the beam dynamics experiments, the accelerator would be used as a test bed for new and special component development which would enhance its operation as well as develop information for HIDE and beyond. A preliminary list of such accelerator elements, subsystems, and components to be considered in the design phase or, later, in the R&D phase is given below:

- 1) A small diameter periodic internal focusing drift tube*
- 2) High field dc superconducting quadrupoles
- 3) Cryopump vacuum system
- 4) Low loss induction accelerator cores
- 5) Final buncher
- 6) Gas stripper and analyzer
- 7) Beam splitter and final focus magnets

*See W.B. Herrmannsfeldt, Heavy Ion Workshop ANL 1978.

- 8) Higher mass ion source (in some respects the Cs^{+1} is similar to U^{+2} , which is a prime candidate for HIDE, but obtaining a U^{+} source is a possible goal).
- 9) Neutralization, plasma transport
- 10) Achromatic bend
- 11) Recirculator

Because the LIA uses a number of individually powered nonresonant accelerating modules, it has the ability to produce many waveforms and accelerate any of the ion species and charge states which have been, or may be, considered. In addition to this flexibility, it may be extended in energy, with a monotonically decreasing cost of the acceleration per energy interval.

Description of 500 Joule Cs^{+1} Test Bed Accelerator

The accelerator consists of a 750 kV, 2.75 Amp Cs^{+1} contact ionization source, two drift tubes driven in a bipolar manner with voltages ≤ 750 kV, and a series of low voltage induction units interspersed with low field quadrupoles (Fig. 1). The acceleration waveform is a flat 750 kV pulse in both the gun and the first drift tube, and at the entrance to the second drift tube. At the exit of the second drift tube and in the first few subsequent induction units the waveform is steeply ramped to generate an energy tilt along the bunch such that the rear particles have a higher energy than the front particles. The relative slope of the applied voltage ramp is decreased to zero as the bunch travels through the accelerator, while the amplitude of the voltage is monotonically increased as the pulse duration decreases (Fig. 2). As the bunch leaves the accelerator, the energy tilt will be further increased, leading to about a factor of three bunching after some drift. Small voltage corrections or "ears" are applied to the voltage waveforms to counteract the longitudinally defocusing field caused by space charge at the ends of the bunch. Because of this space charge effect, a small number of particles will move from the front of the bunch to the rear and vice versa, corresponding to the equivalent of half a synchrotron oscillation, as the bunch travels through the entire machine. Accelerator

parameters and costs, and the current/voltage operating line are shown in Figure 3.

In FY 1979 dollars, a preliminary estimate for the 500 J Cs⁺¹ case lies in the range 16-18 M\$. Adding 25% for EDIA and 25% for contingency, the integrated program cost would be roughly 25-28 M\$. The cost for a 1,700 J, Cs⁺², 47 MeV alternative option has not yet been estimated.

1.2.2 Induction Accelerator Cost Studies and Conceptual Design (E. Hoyer)

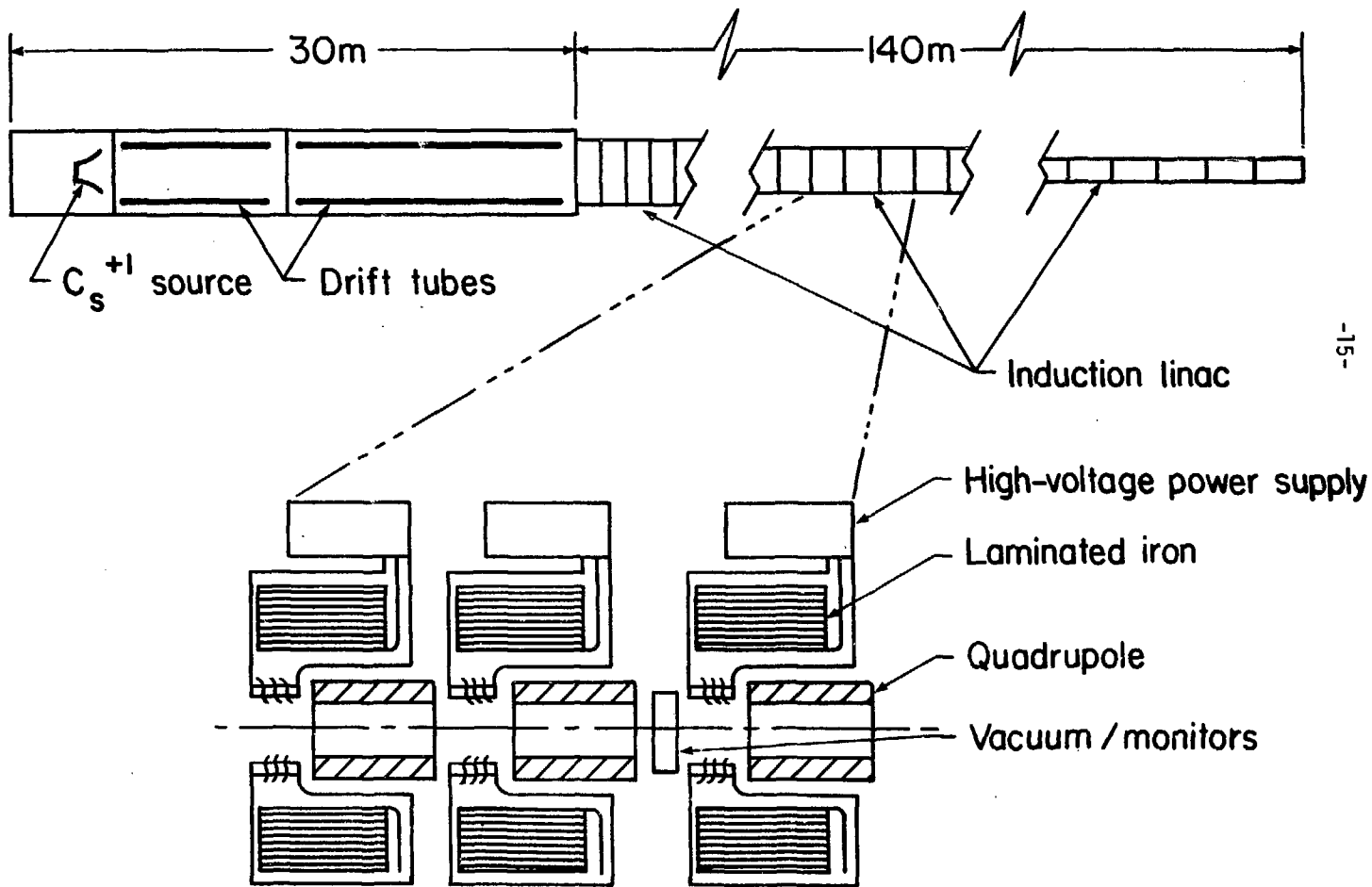
Further development of the Linear Induction Accelerator Cost Evaluation Program (LIACEP) has been carried out. Additional features and changes that have been incorporated in the program include:

- 1) The core excitation voltage can be varied to allow examination of the sensitivity of accelerator costs to core excitation voltage.
- 2) Power requirements for the transport elements are given as an output.
- 3) Stored energy and power requirements for the accelerating modules are calculated and displayed.
- 4) The total cost of a minimum cost accelerator between any two voltage (energy) limits is determined directly in the program.
- 5) Nickel iron as a core material can be examined.
- 6) Core size and dissipation restraints have been revised for pulse durations of less than 500 nanoseconds.
- 7) Dimensional information for accelerator layout is provided.

Much of the engineering input for the LIACEP program has now been documented in LBL Engineering Note M5318.¹

A brief synopsis of the design approach and methodology used in heavy ion fusion induction linac design was presented at the Particle Accelerator Conference in San Francisco, March 1979. The paper entitled Design/Cost Study of an Induction Linac for Heavy Ions for Pellet Fusion is included in Appendix B.

A result of the effort on LIACEP has been a cost reduction in the accelerator portion of the reference design presented at the ANL Heavy



-15-

Fig. 1. 25 MeV Cs^{+1} 500 Joule Induction Linac Test Bed.

XBL 794-1272

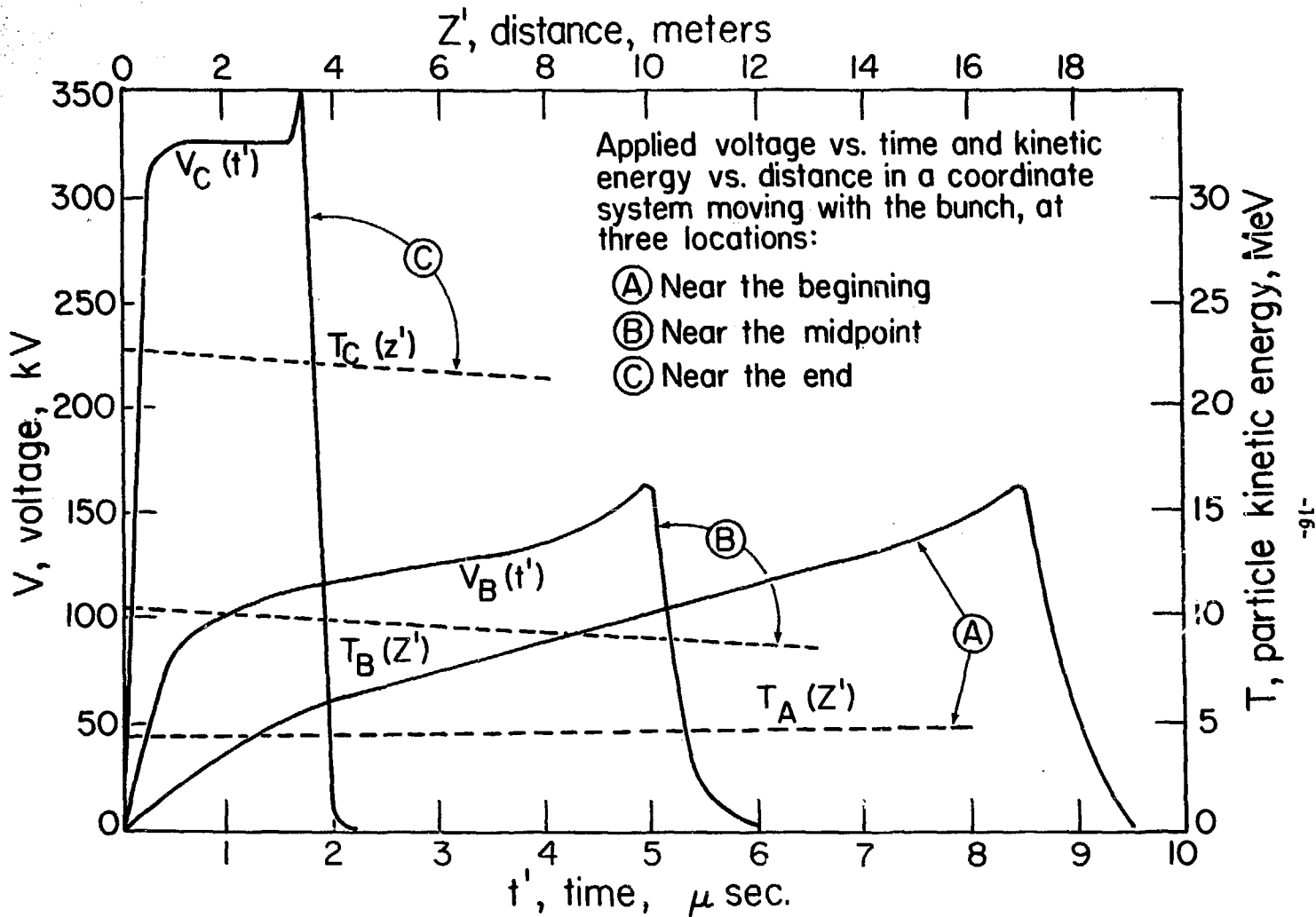
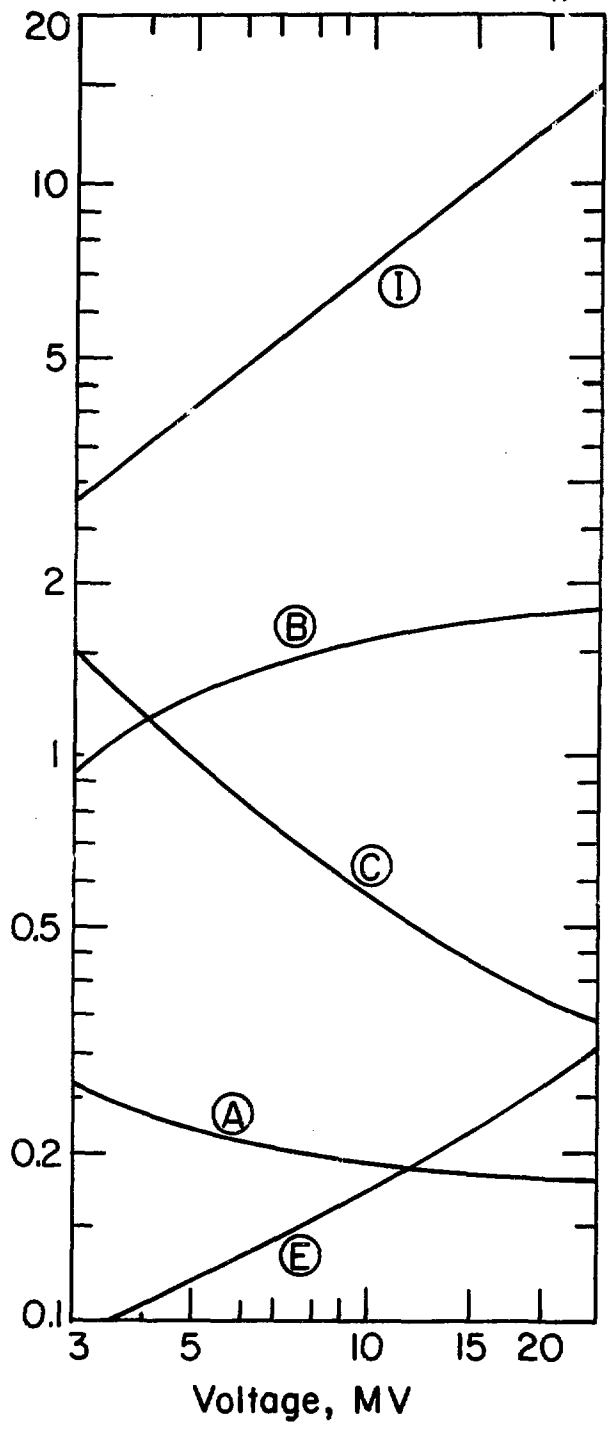


Figure 2



- Ⓐ Aperture, m
- Ⓑ Field, teslas
- Ⓒ Total accelerator incremental cost, \$/volt
- Ⓔ Accelerator gradient, MV/m
- Ⓘ Accelerator current, amps

Figure 3

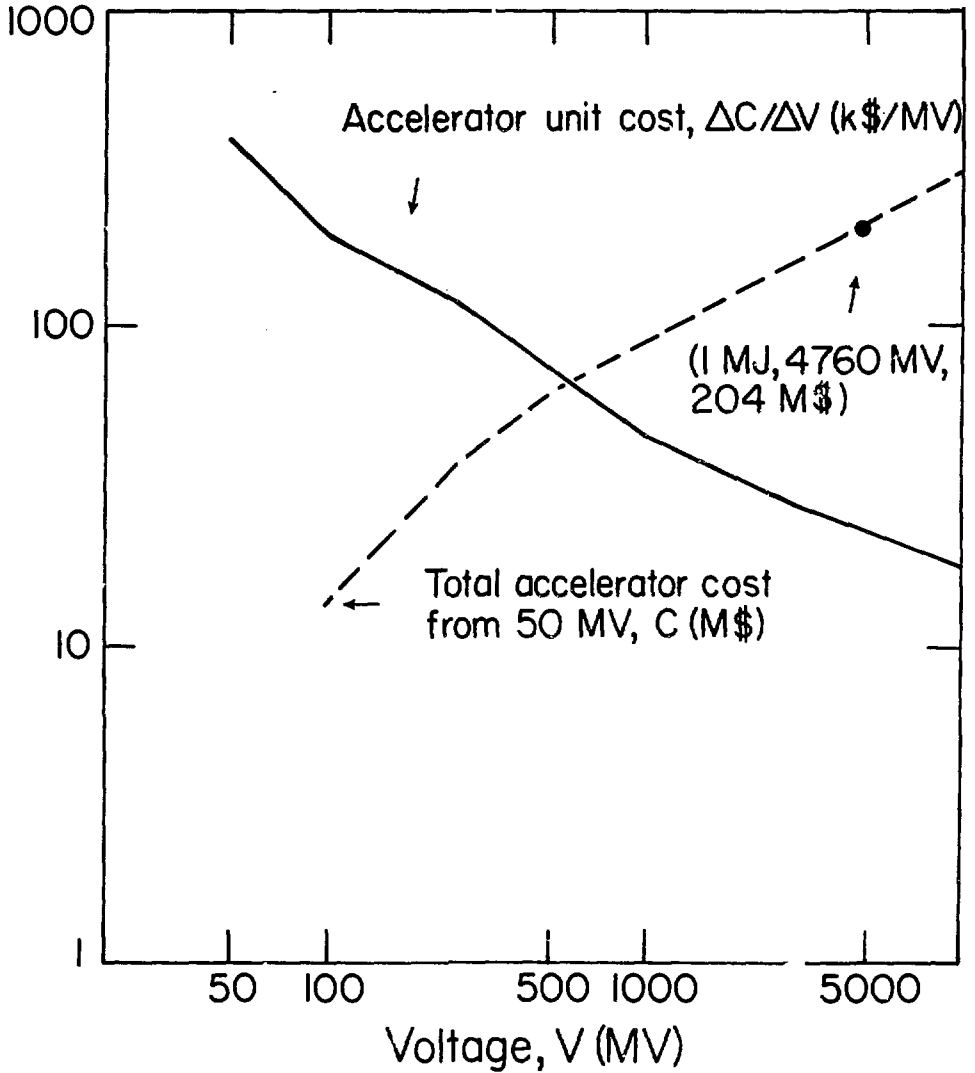
Ion Fusion workshop.^{2,3} We find for this reference case a 30% cost reduction, from 300 M\$ down to 204 M\$ for the accelerator cost (see Fig. 1).

Further, we find the operating curve of current, I , and pulse duration, τ , as a function of voltage (energy) as shown in Fig. 2 to be more favorable--a higher current for the minimum cost accelerator. In particular, the operating curve differs significantly from that reported at ANL^{2,3} in the 2000-5000 MV range. For example, at 4000 MV we now find, for the minimum cost accelerator, a best current of 1200 amps; previously the optimum was 400 amps. Thus one can operate at currents given for the minimum cost accelerator over nearly the entire accelerator voltage (energy) range. As shown in Fig. 2, near the final energy a stronger voltage ramp is applied, increasing the current above the minimum cost accelerator current, to obtain the necessary pulse compression at the target.

One of the features of the LIACEP program is to provide dimensional information for accelerator design. The conceptual sketch, Fig. 3, shows what the reference design might look like at 4000 MV voltage (16 GeV).

References:

1. E. Hoyer, Engineering Input for program LIACEP, Eng. Note M5318, 1979.
2. Proceedings of the Heavy Ion Fusion Workshop, Argonne National Laboratory Report, to be published, April 1979.
3. A. Faltens, E. Hoyer, D. Keefe, L.J. Laslett, A Conceptual Design and Cost Procedure for Heavy-Ion Induction Linacs, LBL-8424 (HI-FAN-60), 1978. Appendix B.



XBL 794-1268

Fig. 1. Accelerator Minimum Unit Cost and Minimum Total Accelerator Cost from 50 MV

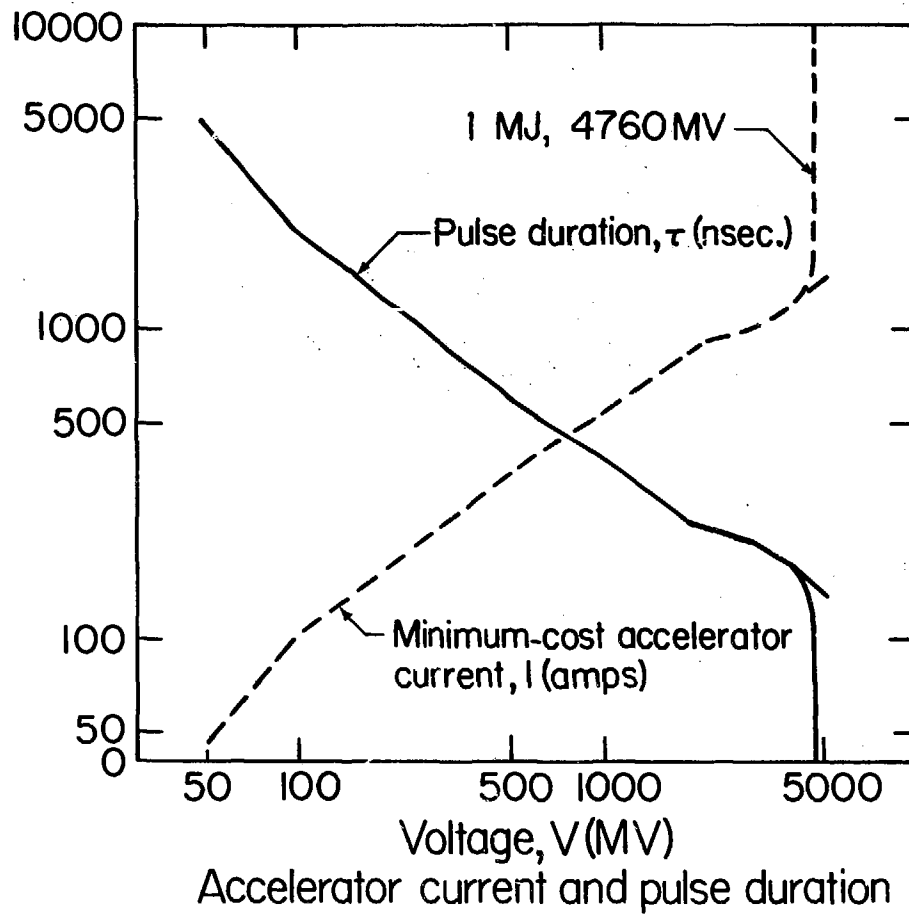


Figure 2

XBL 794-1265

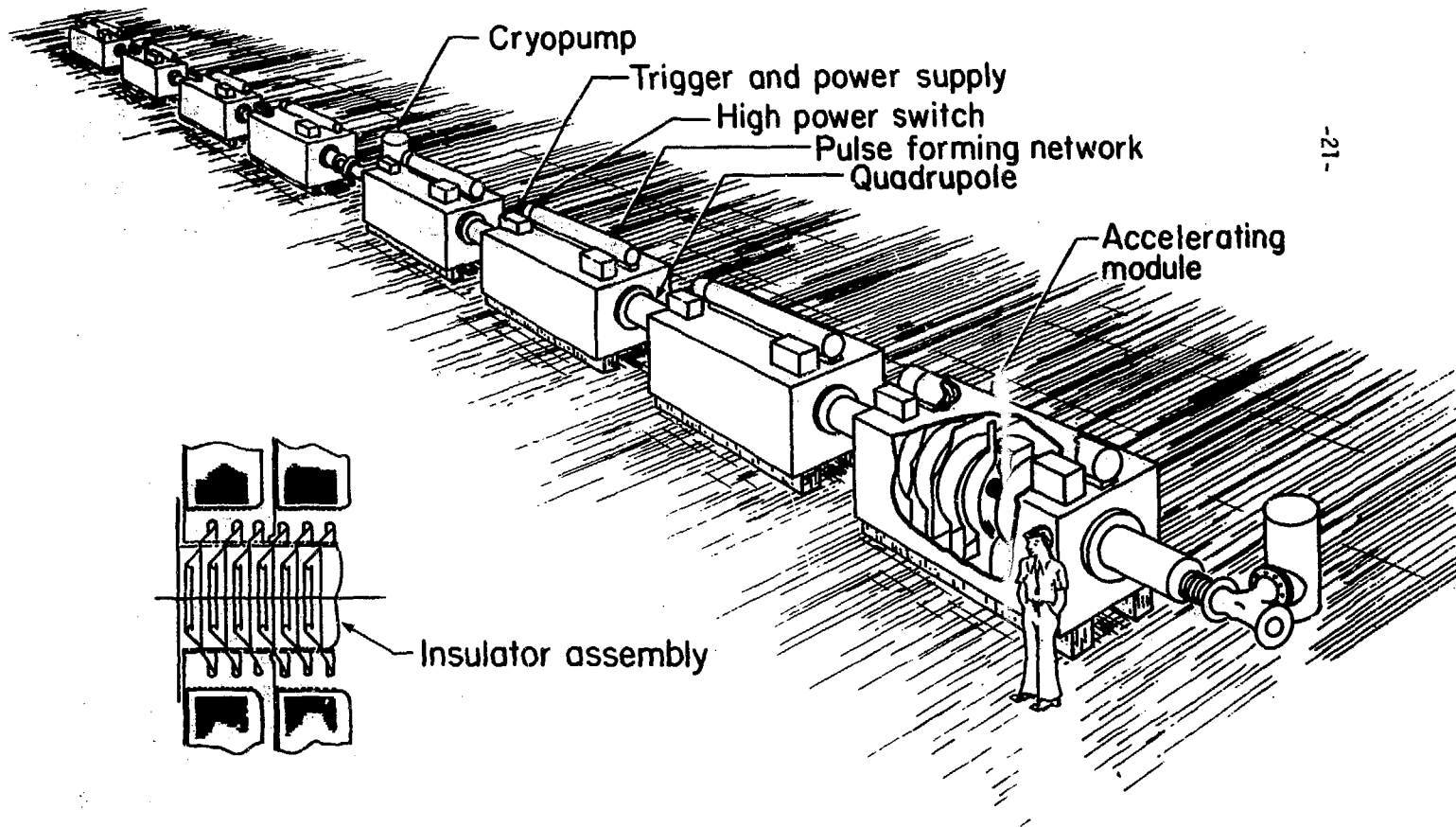


Fig. 3. Induction Linac Heavy Ion Fusion Driver.

XBL 794-1264

1.3 ENGINEERING TESTS

1.3.1 Evaluation of Ferromagnetic Core Materials for the Induction Linac (S. Rosenblum)

Because the magnetic cores make up a large part of the volume and cost of an induction linac it is important to pick the optimum material for the core in terms of its electrical behavior and cost. Because a heavy ion induction linac needs to accelerate over a wide range of pulse widths, several different types of core materials will be necessary.

LBL Test Program

We have, therefore, begun to measure the magnetic properties and core losses of a variety of materials using a thyatron pulser. Each sample is in the form of a tape-wound toroid with a single set of windings. Pulse durations have ranged from 500 ns to 100 μ s thus far. We plan to extend the range down to 40 ns. The materials studied thus far have included .001" thick molybdenum-iron, .001" Ni₅₀Fe₅₀, Stackpole C11 ferrite, .012" Silectron (Arnold Engineering) and three different amorphous magnetic materials--Allied Metglas 2826 and 2826 MB as well as General Electric Fe₈₂B₁₅Si₃.

These latter new materials show great promise, being inexpensive to manufacture (50¢/lb., projected) as well as having very attractive properties as a core material to replace Ni₅₀Fe₅₀ (\$10 - 20/lb.). Although the experimental materials tested thus far have not reached the expected performance based on short sample measurements it is hoped that improvements in fabrication will lead to this result shortly.

Overall View of U.S. Efforts in Amorphous Magnetic Materials

At present there is great interest in the Fe₈₂B₁₅Si₃ material (called Metglass 2605S by Allied Chemical) for use in motors and power distribution transformers because of the low manufacturing cost, good magnetic properties and low electrical losses.

Both Allied Chemical and General Electric have corporate research programs to develop these materials for this market. The Allied program

is the more ambitious, being partly funded by a \$6 million, 3½ year contract (in conjunction with Westinghouse) from the Electric Power Research Institute. Allied can presently produce 50-100 pounds of ribbon a month and is now constructing a pilot plant, which is expected to come on line in August, 1979. This pilot plant will increase the capacity at least by a factor of 10.

General Electric has a more modest program in the production of ribbon material which is totally internally funded; they do all their own materials fabrication and testing. They also have a large effort, partly funded under DOE contract, to develop flaked amorphous magnetic material for the motor-transformer application.

The ribbon material, as it can now be produced, would be acceptable for a part of our core materials needs. We are keeping in close contact with GE and Allied directly as well as through Carl Cline at LLL who is supervising a program in the development and testing of these materials for switching and accelerator applications.

Since the transformer-motor market expects to need some 160 million pounds/year, the total amount required for an HIF induction linac would be a tiny fraction of this. Thus, HIF needs would not require any major new production capacity.

1.3.2 Pulse Power Electronics Engineering Tests (S. Rosenblum)

Measurements are nearing completion on a test setup consisting of two complete induction modules with associated triggering electronics which have been left in place in Building 58 since the time when the other ERA components were dismantled. Among the measurements made were:

- i) careful calibration of cavity capacitive divider
- ii) delay and time jitter between two cavities triggered simultaneously over a range of trigger and charging voltages far from the nominal operating point
- iii) delay in erection time and jitter in erection time for a Marx generator as a function of trigger voltage and charge voltage.
- iv) measurement of wear rate and firing jitter of trigger electrodes of several thicknesses.

A report will be prepared on the results which will be useful in the design of components of the HIF induction linac.

PART II ACTIVITIES RELEVANT TO R.F. LINAC/STORAGE RINGS SYSTEMS

2.1 HIGH-CURRENT Xe⁺¹ ARC SOURCE

2.1.1 Xenon Ion Source (W. Chupp)

A multi-filament multi-aperture Xe⁺¹ Ehlers type plasma arc has been developed and successfully operated. An array of 13 holes symmetrically arranged in a 25 mm diameter circular pattern typically produces a beam of 60 mA at an extraction voltage of 23-25 kV (see Appendix C).

2.1.2 500 kV Xe⁺¹ Beam (W. Chupp)

The multiaperture Xenon source was installed in a 500 kilovolt Cockcroft-Walton terminal and successfully operated early in FY 1979. A 35 mA beam of 500 kV Xe⁺¹ ions was magnetically analyzed and was found to consist of > 90% charge state one (see Appendix C).

2.2* R-F LINAC SYSTEMS

The work summarized in this section concerns questions of low- β heavy-ion acceleration in r.f. linacs and is of direct relevance to the design of the front section of linacs for ion-fusion drivers.

2.2.1* Wideröe r.f. Linac Design (J. Staples, H. Lancaster, R. Yourd)

The Wideröe structure seems, at present, to be a prime candidate for consideration as the low- β part of a heavy-ion driver based upon the r-f linac approach. Although the concept, and its first demonstration, is fifty years old only one significant and highly successful example is in operation today at the GSI Laboratory in Darmstadt, West Germany.

*This work was supported in large part by the HENP Division of the U.S. D.O.E., in connection with the improvements to the SuperHILAC and Bevalac facilities at LBL.

Under construction at this time at LBL is a Wideröe linac as part of a line-item improvement project for the Super HILAC-Bevalac facility. It will operate at 23 MHz, accelerate particles with $q/A \approx 0.02$ (viz., U^{+5}), and have a space charge limit of some 10 emA. These parameters are not far--perhaps a factor of two to four--from those needed for a heavy-ion driver, which could be in the range 6 MHz, $q/A \approx 0.01$, and $I \sim 40$ emA.

The details of the LBL Wideröe linac now under construction are given in Appendix D, a paper by Staples, Lancaster, and Yourd of LBL.

2.2.2* Emittance Growth in r.f. Linacs (Staples, Jameson)

In any accelerator driver system a major preoccupation is with how small a volume of 6-D phase space the needed number of particles will occupy. Key questions concern the dilution of phase space because of three effects--(a) mishandling of the beam in a real-life situation, (b) non-linearities in the externally imposed fields, and (c) non-linearities in the collective self-fields of the beam.

The paper appended in Appendix E by Staples (LBL) and Jameson (LASL) is an attempt to update the effects defined under (b) and (c) above based upon incorporating previous studies in this field.

2.2.3* Future Plans for High Energy Heavy Ion Facilities (C. Leeman)

Designs for high-energy heavy-ion facilities have begun to proliferate around the world. These are reviewed by C. Leeman (LBL) in a paper included as Appendix F. Despite the differences between the requirements for heavy-ion research accelerators and heavy-ion drivers, Leeman's review paper is of particular interest in cataloging the variety of approaches being pursued by the different design groups. In many respects, e.g., with respect to the injection system, the design choices are found to span quite a narrow range.

*This work was supported in large part by the HENP Division of the U.S. D.O.E., in connection with the improvements to the SuperHILAC and Bevalac facilities at LBL.

2.3* ION-ION CROSS-SECTION (Cs^+ , Cs^+) EXPERIMENT
(K. H. Berkner, R. V. Pyle, K. R. Stalder)

The ion-ion charge-exchange cross sections ($X^+ + X^+ \rightarrow X^0 + X^{++}$) and ionization cross sections ($X^+ + X^+ \rightarrow X^+ + X^{+n} + (n-1)e^-$) at energies up to 300 keV must be known to predict the behavior of dense beams of heavy ions to be used in certain heavy ion fusion concepts. Because of relative motions between ions, these reactions can take place and change the charge, resulting in loss of beam. At the ERDA Summer Study of Inertial Fusion (1976) Cs^+ was discussed as a possible beam candidate. It is still a good candidate. At the conclusion of the Argonne Workshop (Sep. '78) the atomic cross-sections working group concluded that their theoretical studies on many different ion species could best be calibrated by measurements with cesium ions.¹

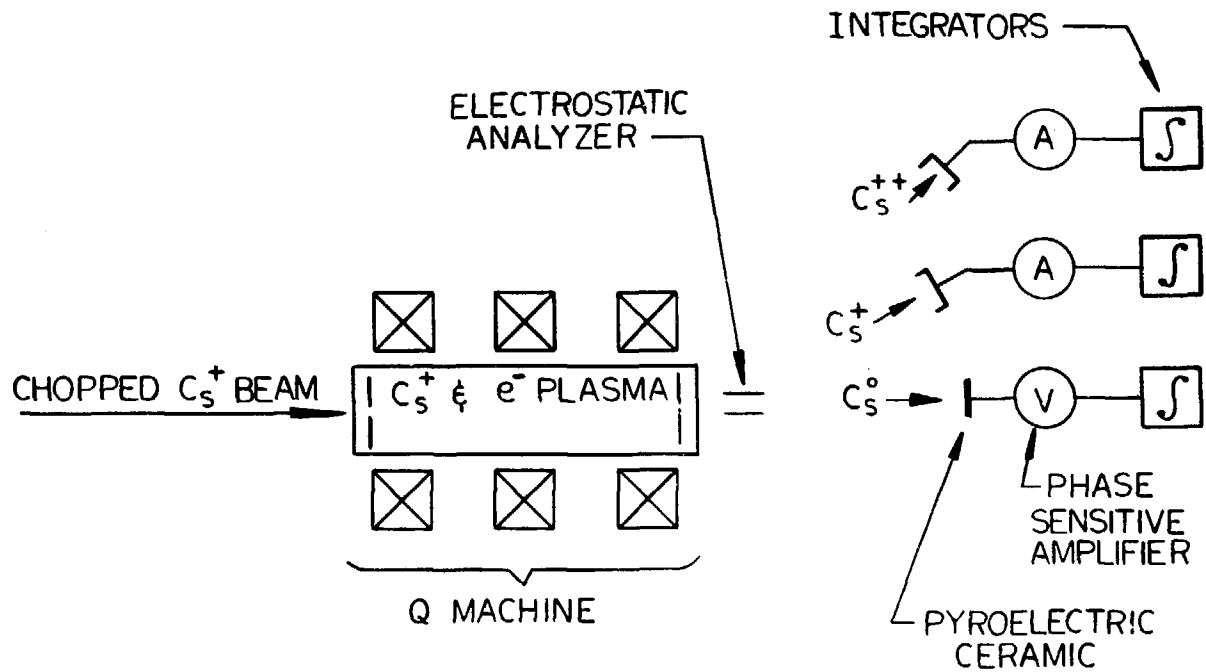
We are setting up an experiment to measure the $Cs^+ + Cs^+ \rightarrow Cs^0 + Cs^{++}$ and $Cs^+ + Cs^{+n} + (n-1)e^-$ cross sections. A beam of 10- to 300-keV Cs^+ ions will be transmitted through a Cs^+ target plasma (Q machine), and the cross-section will be determined from the growth of the Cs^0 and Cs^{+n} components of the beam as a function of the Cs^+ target density (Fig. 1).

The Q-machine had been partially fabricated for use in a $D^- + Cs^+$ experiment when funding for the $Cs^+ + Cs^+$ experiment was received in December 1978. It was decided to postpone the D^- experiment and accelerate the schedule so that preliminary $Cs^+ + Cs^+$ results could be obtained in about nine months (see Fig. 2).

Progress in the past four months includes:

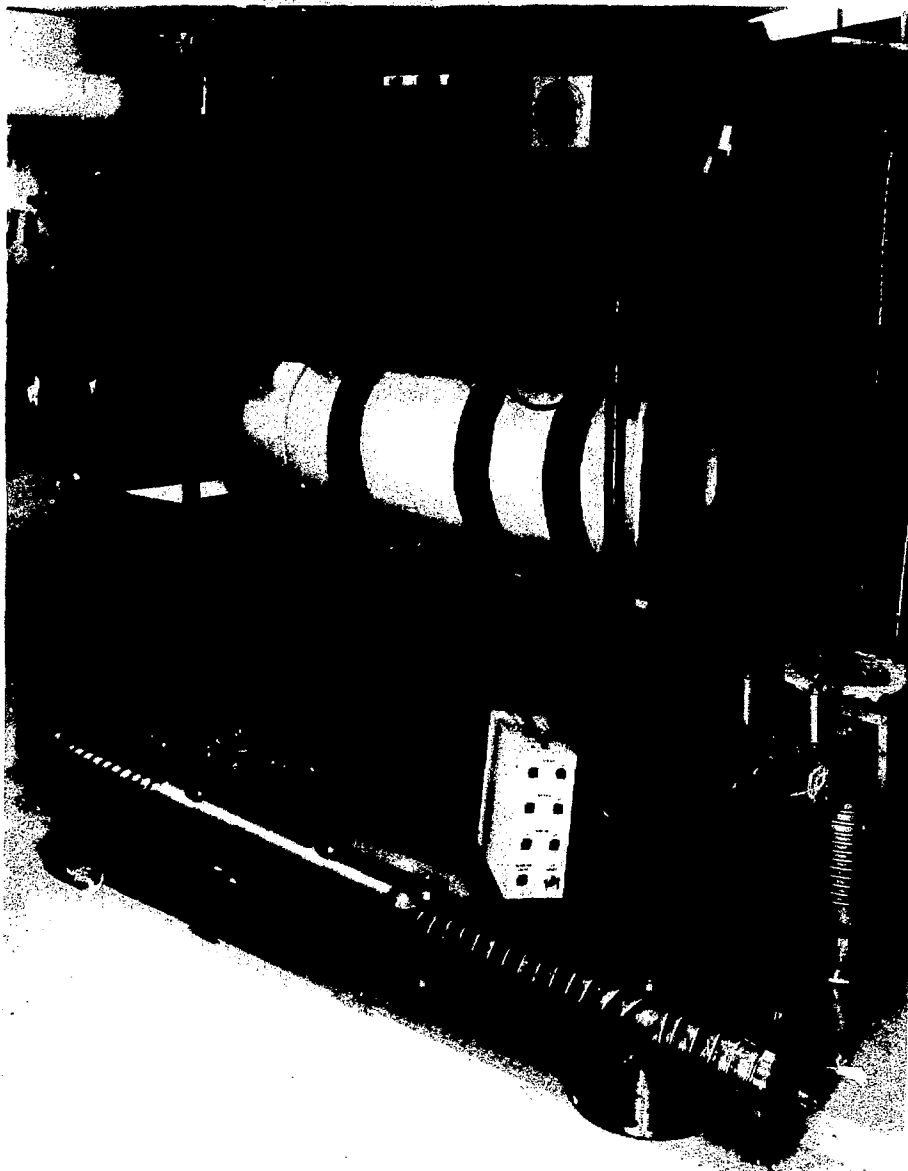
1. Cs^+ Ion Source - A Cs^+ ion source suitable for mounting on our research accelerator has been fabricated. Tests are scheduled to start in April.
2. Accelerator - A 150 kV research accelerator is available for initial tests. This will be converted to 300 kV in May or June.
3. Momentum Analysis Magnet - A magnet suitable for Cs^+ analysis has been installed and checked out on the beam line.

*Supported by LBL Director's Program Funds.



EXPERIMENTAL ARRANGEMENT FOR DETERMINATION OF
 $Cs^+ + Cs^+ \rightarrow Cs^{++} + Cs^0$ CROSS SECTION

Figure 1



BBC-786-7745

Fig. 2. Cs^+ Q-Machine

4. Q-machine target - A refrigeration system has been installed. A Cs^+ plasma has been produced. Plasma-diagnostic development is continuing. An improved Cs oven has been fabricated, but not checked out.
5. Beam analysis chamber - Fabrication of an analysis chamber has started. Completion is expected in June.

If no problems are encountered with the Cs^+ source, we should have transported a Cs^+ beam through the Q-machine by May. The analysis chamber will be installed in June and checkout of the complete system will start in July.

References:

1. R. Macek, Y-K Kim (private communication, Oct. 1978).

PART III THEORY

3.1 THEORY (L. Smith)

At the time of the Argonne Workshop (Sep. '78), we had made a preliminary comparison of our analytic work on a third-order instability which occurs in the transport of a Kapchinskij-Vladimirskij beam through a quadrupole system with some of the results of Irving Haber's particle simulation calculation of the same instability. We were encouraged to believe that theory and computation were in agreement, but there remained a number of gaps and unresolved questions. Since then we have obtained the complete record of that run and find that over a range of about ten quadrupole periods, after the instability has grown out of the computational noise and before signs of non-linear saturation appear, the relevant moments of the distribution grow at the predicted rates to a remarkable accuracy. We are therefore quite confident in our double conclusion that the theory is correct and that the simulation computations are correct. It should then be justifiable to believe the computational results also for more realistic initial distribution functions, which are beyond the capability of analytic treatment.

Our analytic work thus indicates that the maximum current that can be transported without emittance degradation is achieved by using a lattice designed for a zero intensity phase advance of 60° (to avoid envelope and third order instabilities), depressed to $\sim 24^\circ$ by space charge forces (the threshold for higher order instabilities). This criterion should be conservative, since the K-V distribution is somewhat more sensitive to instability than other more realistic distributions. The corresponding "figure of merit," $Q/u_m^{2/3}$, in the formula for current given in equation (3) of reference (1) depends on the fraction of transport channel occupied by quadrupoles, ranging from 0.76 for full occupancy down to 0.23 for 10% occupancy (see Appendix G; Ref. 2). This coefficient is not drastically different numerically from that proposed by Maschke at the time of the first HIF workshop.

What is needed now to advance the study of beam transport is an analysis of the three dimensional problem, including longitudinal forces and the resulting coupled motion. As a first step in that direction,

we are using a one-dimensional code for longitudinal motion and developing an analytic approach to that problem. A distribution function has been found for which the space charge forces are linear and which leads to an envelope equation similar to the familiar one for transverse motion (see Appendix H). A perturbation analysis shows that this distribution is stable at all intensities if the (linear) external focusing force is continuous. The analysis is being extended to the case of discontinuous external forces, a situation that is more realistic. We anticipate that instabilities will be found; the question is whether or not they will occur in parameter ranges of practical interest. The computer code has been applied to the final compression process for parameters corresponding to an induction linac scenario and for a variety of plausible distribution functions. Within the limitation of a one-dimensional model, the process seems to go satisfactorily; the results can be described approximately by an envelope equation using a suitably defined longitudinal emittance.

References:

1. G. Lambertson, L.J. Laslett, L. Smith, Proceedings of the 1977 Particle Accelerator Conference.
2. L.J. Laslett, L. Smith, Proceedings of the 1979 Particle Accelerator Conference.

PART IV OTHER ACTIVITIES

4.1 THE COST OF HIF POWER (W. B. Hermannsfeldt)

The cost of electricity from a capital-intensive facility, such as a fusion power plant, is dominated by the capital charges which can be found from

$$C_e = C_t \times R / (365 \times 24 \times C_f \times P_n) \quad (1)$$

where

C_t = total capital cost of the plant,

R = Annual fixed charge rate,

C_f = Capacity factor, and

P_n = Rated net power of the plant.

The net power of the plant is found from

$$P_n = (1 - f) P \quad (2)$$

where

P = Total electrical power generated, and

fP = Recirculating power to the driver.

Note that

$$fP = nE/\eta$$

where

E = Driver energy per pulse,

n = Pulse repetition rate, and

η = Electrical conversion efficiency of the driver.

The total power generated is given by

$$P = fP_n g \epsilon \quad (4)$$

where

g = Pellet gain, and

ϵ = Thermal conversion efficiency of the turbine plant.

Substituting Eqs. (2) - (4) into Eq. (1) yields

$$C_e = \frac{C_t R \eta}{8760 \times C_f (ng\epsilon - 1) n E}$$

The total cost of electricity is found by adding fuel charges and operating costs to the expression in Eq. (5). In the following examples, it will be assumed that these costs add 10% to the total cost of power. (Light water reactors (LWR) usually estimate about 5% for operation.)

Reasonable values, typically used by industry for finding the cost of power are: $R = 15\%$, $C_f = 65\%$ and $\epsilon = 33\%$. Substituting these values into Eq. (5), and expressing the result in mills/kWh, we find

$$C_e(\text{mills/kWh}) = \frac{26300 C_t(\$B)\eta}{(\eta g/3-1) n(s^{-1}) E(\text{MJ})} \quad (6)$$

The pellet gain as a function of driver energy has been calculated for various pellet designs by R. Bangerter at LLL. The function

$$g = 200 (E^{0.4} - 0.5) \quad (7)$$

describes the pellet gain for a class of single shell targets. A more conservative function would be to take half of the values given by Eq. (7) while if one assumes double shell targets, the results could be double that of Eq. (7). These functions are shown plotted in Fig. 1.

There now remains only the task of estimating C_t , the cost of the power plant, to be able to calculate the cost of ICF power as a function of driver energy and efficiency. The cost of the driver can be estimated from the studies made by E. Hoyer et al of LBL. The expression $C_D(\$B) = 0.7E^{0.4}$ approximately fits Hoyer's data when the conventional indirects used by utility companies are included, i.e., engineering, contingency and interest on the capital expended during the construction period. The total cost of the plant must include the driver, the reactor system including all the steam to electric conversion equipment, and the special equipment related to the pellets including the tritium handling equipment. The cost of a LWR is dominated by conventional turbines, cooling towers, etc., so that unless the nuclear steam supply system (NSSS) of a fusion plant is more than double the cost of the NSSS for a LWR, the effect on power cost is very small. We will assume that the cost of a 1GWe fusion plant, not including the driver and pellet facilities, is the same as that of a 1 GWe LWR, about \$1 billion. An

additional \$0.2 billion is added for the pellet factory, making the total

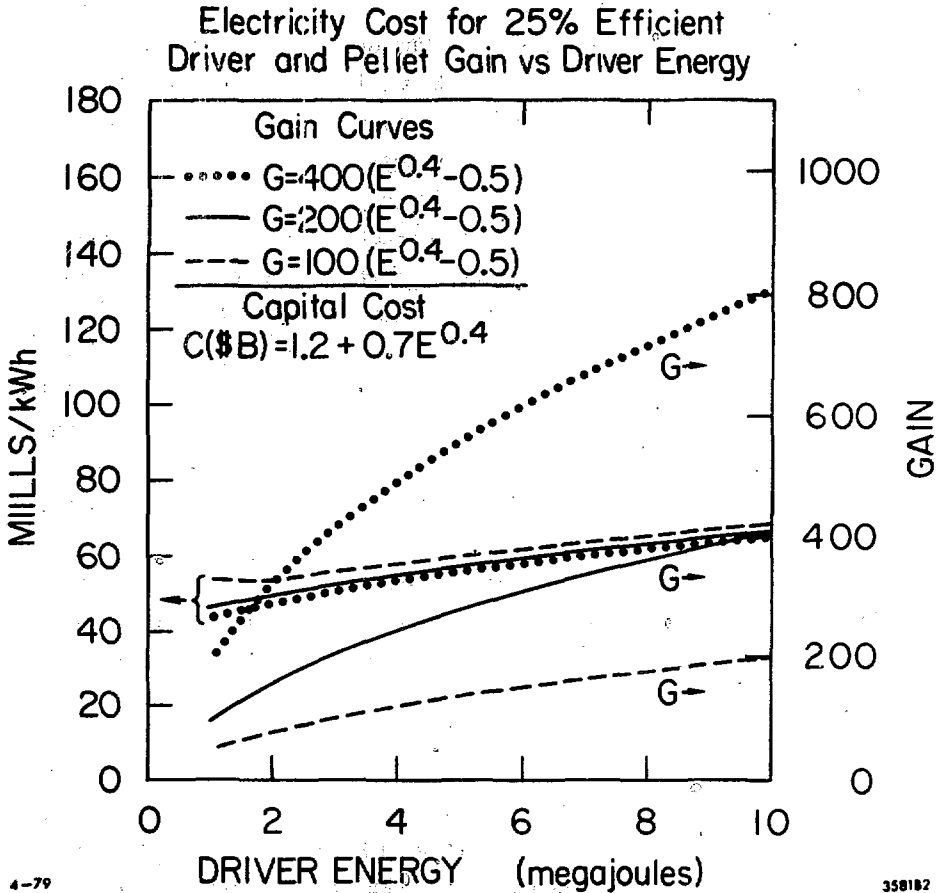
$$C_t (\$B) = 1.2 + 0.7E^{0.4}$$

The cost curves in Fig. 1 show the resulting cost of electricity for a 25% efficient driver, including the 10% for operating. The remarkably flat cost function, especially for $E \leq 5$ MJ, is due to the rising gain curve offsetting the rising cost of the driver as a function of energy. It is also noteworthy that the resulting cost of electricity is nearly independent of pellet gain for high efficiency drivers.

Note that to keep power output independent of driver energy and pellet gain, it is necessary to assume that the pulse repetition rate can be varied at will. For the curves plotted, the repetition rate varies from ~ 40 Hz at 1 MJ down to about 1 Hz at 10 MJ. If the lower gain curve is used, these values must be doubled. Pellet costs, pellet injection techniques, driver repetition rate and other factors must be considered when such high repetition rates are contemplated. On the positive side, the cost of the reactor vessel is expected to be reduced for higher repetition rate, lower yield explosions.

The significance of driver efficiency is shown explicitly by the curves in Fig. 2. For lower efficiency drivers, the recirculating power increases rapidly. The rule of thumb that the product ηg must be ≥ 10 only works so long as the product Eg remains below some realistic value. We consider an absolute upper limit on Eg to be about 4000 MJ, equivalent to about one ton of high explosives!

The resulting range of power costs, about 45-60 mills/kWh, are the cost in FY1979 dollars for plants built with FY1979 dollars. Making the same assumptions, coal power would cost about 44 mills/kWh and LWR nuclear power about 33 mills/kWh. The relatively higher rate of inflation for fuel costs means that in the very near future, coal would be more expensive than fusion. Assuming that uranium costs rise 3% faster than general inflation, by about the year 2010 LWR nuclear power would also cost more than fusion power.



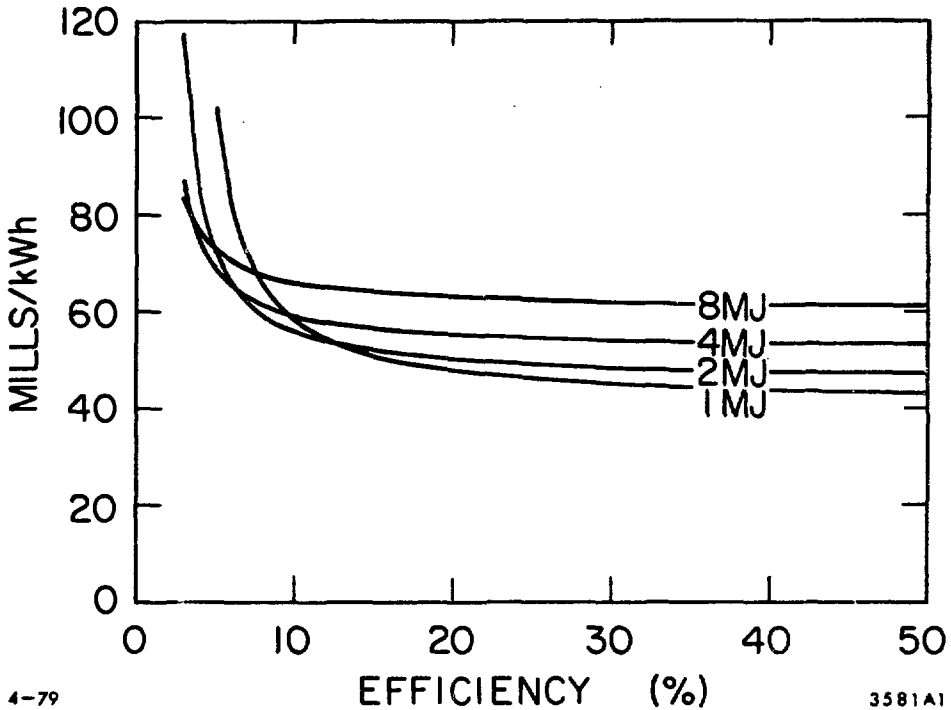
4-79

358182

XBL 794-9376

Fig. 1. Electricity cost for 25% efficient drivers is shown plotted as a function of driver energy. The assumptions include the pellet gain as a function of energy, which is also shown, and the capital cost function of the entire facility. A 10% increment for operation has been included.

Electricity Cost vs Driver Efficiency for $G=200 (E^{0.4}-0.5)$



4-79

3581A1

XBL 794-9375

Fig. 2. Electricity cost as a function of efficiency is shown using the same cost assumptions given for Fig. 1.

4.2 COMPLETION OF HIGH-BAY EXTENSION (W. Chupp)

An addition to Building 58A which houses the $1A \text{ Cs}^{+1}$ contact ionization source is scheduled for completion in early April. This will add 1600 square feet to the high-bay area and will expedite the assembly and installation of the pulsed drift tube system.

PART V HEAVY ION FUSION NOTES

5.1 REPORTS INDEX (10/1/78 - 3/31/79)

Number	Author	Title	Date
HI-FAN-56	L.J. Laslett	Concerning an A-G Transport System with $\sigma_0 = 60$ Degrees	10/78
HI-FAN-57 (LBL-8304)	D. Neuffer (HIF Workshop)	Geometric Aberrations in Final Focussing for Heavy Ion Fusion	10/78
HI-FAN-58	HIF Staff	Linear Induction Accelerator Conceptual Design	9/6/78
HI-FAN-59	L.J. Laslett	Letter to Dr. Ingo Hofmann - dated 10/25/78	10/25/78
HI-FAN-60 (LBL-8424)	HIF Group	Year-End Report - Fiscal Year 1978	10/30/78
HI-FAN-61 (LBL-8353)	A. Garren (HIF Workshop)	Summary of the Working Group on High Current Transport and Final Focus Lenses	10/78
HI-FAN-62 (LBL-8351)	L.J. Laslett, I. Haber, L. Smith (HIF Workshop)	Comparison of Instability Theory with Simulation Results	10/78
HI-FAN-63 (LBL-8494)	D. Keefe, et al (HIF Workshop)	Status Report on the Lawrence Berkeley Laboratory Heavy Ion Fusion Program	10/78
HI-FAN-64	L.J. Laslett	Moments at Half-Period Points	12/18/78
HI-FAN-65 (LBL-7591)	HIF Group	Half Year Report on the LBL HIF Program	3/31/78
HI-FAN-66	HIF Group	Informal Quarterly Report on LBL HIF Program	4/1-6/30 1978
HI-FAN-67	HIF Group	"One-Kilojoule" Induction Linac Test Bed	1/16/79
HI-FAN-68	HIF Group	Informal Quarterly Report on HIF Program	10/1-12/31
HI-FAN-69 (For internal use only)	L.J. Laslett	Stability of a Kapchinskij-Vladimirskij Beam in a Continuous-solenoid Transport System	1/19/79

Number	Author	Title	Date
HI-FAN-70 UCID-8105	David Neuffer	A Self-Consistent Phase Distribution with an Envelope Equation for Longitudinal Motion	1/79
HI-FAN-71	W. Herrmannsfeldt	The Economics of ICF Power	2/9/79
HI-FAN-72	David Neuffer	Normal Modes of the Stationary Longitudinal Distribution	3/79
HI-FAN-73 (LBL-8359)	C. Kim, D. Keefe	Large Aperture Contact Cs ⁺¹ Ion Source for an Induction Linac	3/79 (PAC paper)
HI-FAN-74 (LBL-8357)	D. Keefe	Design/Cost Study of an Induction Linac for Heavy Ions for Pellet-Fusion	3/79 (PAC paper)
HI-FAN-75 (LBL-8859)	W. Chupp, J. Staples	Operation of a High-Current Xenon Source	3/79 (PAC paper)
HI-FAN-76	Lloyd Smith	MEMO to Terry Godlove: Evaluation of the State of the Art of Accelerators as Heavy Ion Drivers	3/79
HI-FAN-77 (LBL-8387)	D. Neuffer	Longitudinal Motion in High Current High Energy Heavy Ion Beams	3/79 (PAC paper)
HI-FAN-78 (LBL-8382)	L.J. Laslett, L. Smith	Stability of Intense Transported Beam	3/79 (PAC paper)
HI-FAN-79	Ingo Hofmann	Influence of the Distribution Function on Eigenoscillations and Stability of a Beam	12/78
HI-FAN-81 (SLAC-PUB-2201)	W.B. Herrmannsfeldt	A Charge Separating Spectrometer for Annular Ion Beams	11/78
HI-FAN-82 (SLAC-PUB-2196)	W.B. Herrmannsfeldt	A Multi-Ampere Heavy Ion Injector for Linear Induction Accelerators Using Periodic Electrostatic Focusing	11/78

PART VI APPENDICES

- A. S. Abbott, et al, "Large-Aperture Contact-Ionized Cs⁺¹ Ion Source for an Induction Linac," LBL-8359, 1979 Particle Accelerator Conf., San Francisco, March 12-14, 1979.
- B. A. Faltens, et al, "Design/Cost Study of an Induction Linac for Heavy Ions for Pellet-Fusion," LBL-8357, Ibid.
- C. W. Chupp, et al, "Operation of a High Current Xenon Source," LBL-8859, Ibid.
- D. J.W. Staples, et al, "A Wideröe-Based Heavy Ion Preaccelerator for the Superhilac," LBL-8810, Ibid.
- E. J.W. Staples, R.A. Jameson, "Possible Lower Limit to Linac Emittance," LBL-8809, Ibid.
- F. C. Leemann, "Prospects for High Energy Heavy Ion Accelerators," LBL-8899, Ibid.
- G. L.J. Laslett, L. Smith, "Stability of Intense Transported Beams," LBL-8382, Ibid.
- H. D. Neuffer, "Longitudinal Motion in High Current Ion Beams-- A Self-Consistent Phase Space Distribution with an Envelope Equation," LBL-8387, Ibid.

APPENDIX A

LARGE APERTURE CONTACT IONIZED Cs⁺¹ ION SOURCE FOR AN INDUCTION LINAC*

Steven Abbott,⁺ Warren Chuupp,⁺ Andria Faltens,⁺ William Herrmannsfeldt,⁺⁺
Egon Hoyer,⁺ Denis Keefe,⁺ Charles Hongchul Kim,⁺
Stephen Rosenblum,⁺ and Joseph Shilon⁺

Abstract

A 500 KeV one-ampere Cs⁺¹ ion beam has been generated by contact ionization with a 30 cm dia. iridium hot plate. Reproducibility of space charge limited ion current wave forms at repetition rates up to 1 Hz has been verified. The beam is characterized to be very bright and suitable as an ion source for the induction linac based heavy ion fusion scheme. The hot anode plate was found to be reliable and self-cleaning during the operation.

Introduction

Among the leading accelerator driver technologies for heavy ion fusion, only the linear induction accelerator technology has the advantages of being a single-pass high repetition rate accelerator without requiring current amplification by storage rings at the end. One of the major problems in the application of the linear induction accelerator technology has been that of finding a suitable injector which could deliver of the order of a few hundred micro-coulombs of heavy ions within a normalized emittance of $\epsilon_N = 2 \times 10^{-5}$ radian-meters for the one MJ reference design. A. Faltens and D. Keefe proposed to use the pulsed drift tube acceleration method for the injector.⁽¹⁾ An R/D program was initiated at LBL to develop a suitable ion source and to demonstrate the drift tube and induction linac technologies for heavy ions.⁽²⁾ The purpose of the present paper is to describe the status of the R/D program.

A contact-ionization⁽³⁾ ion source was chosen because; (1) it is in principle very bright (very dense in six dimensional phase space), (2) it has very low intrinsic background impurities (very high fractional ionization of >99%, singly ionized), (3) it is scalable up to a few hundred μC easily, and (4) it may in the future be applicable to uranium.⁽⁴⁾

A large aperture (30 cm dia.) Pierce geometry pulsed cesium contact-ionization source was constructed and operated at full design voltage of 0.5 MV single-gap and has delivered the full design current of more than 1 ampere. A three section pulsed drift-tube linac is being assembled which will accelerate the Cs⁺¹ beam to 2-3.5 MeV depending on whether the drift-tube linac is operated in the uni-polar or in the bi-polar mode.

Experimental Apparatus

A schematic diagram of the experimental setup is shown in Fig. 1. Neutral Cs⁺¹ atoms are sprayed onto the hot iridium plate (anode) of 30 cm dia. which is at a temperature of 1200° K - 1400° K. Most of the cesium atoms are adsorbed on the surface⁽³⁾ as ions while some of them are emitted.

*This work was supported by the Office of Inertial Fusion of the U.S. Department of Energy under contract No. W-7405-ENG-48.

+Lawrence Berkeley Laboratory, Berkeley, Calif. 94720
++SLAC, Palo Alto, Calif. 94305.

The emission rate is dependent upon the fractional coverage of the anode with Cs atoms and on the temperature of the anode.⁽³⁾ In space charge limited operation, where the Child-Langmuir current is smaller than the emission limit, the beam is uniform in the transverse direction, insensitive to the non-uniformities of the anode temperature and of the Cs coverage. High voltages up to 500 kV were applied to the anode by the Marx generator. The pulse length is variable, being determined by the firing of the crow bar spark-gap.

The source tank is pumped by a liquid helium cryopump and several diffusion pumps to 2×10^{-7} Torr. The partial pressure of Cs vapor was measured to be less than 10^{-8} Torr, with a residual gas analyzer. The partial pressure will be reduced further by using a pulsed Cs arc vapor source.

Each of the three drift tubes will have one, and eventually two Marx generators identical to the 500 kV anode Marx generator. The beam is focussed electrostatically with Pierce electrodes at the emitter and grids in the accelerating gaps. In normal operation the Cs surface coverage is determined by the pump uptake and the source supply rates.

In normal operation the iridium plate and surrounding electrodes are self-cleaning. The equilibrium coverage of Cs on various electrodes and insulators is controlled by the local temperature, the supply rate of Cesium, and the pumping rate of Cs by various cold surfaces and pumps. With only the DP and turbo-molecular pumps working, the Cs leaves the system in the time scale of a day; with the cryopump and its LN and water baffles operating, the Cs leaves the system in less than one hour. With extreme over-supply of Cs the voltage hold-off capability of the system is lowered to approximately one-third of its peak value, and in such circumstances it is faster (1 day) to dismantle the system and wash it with water than to let it recover by itself.

Experimental Results

Typical voltage and current waveforms are shown in Fig. 2. The voltage was measured with a calibrated capacitive divider and the current was measured with a small shielded probe. Time of flight measurements showed that virtually all the beam was composed of singly ionized cesium ions (Fig. 3).

The total Cs⁺¹ current was measured with a 15" dia. Faraday cup which had two highly transparent biased screens to suppress the effects of electrons in measuring the current. The first screen close to the iridium hot plate was biased at ground potential, while the second screen was biased at -600 volts to repel any electrons which may travel with the beam. The collector was biased to +300 volts to retain the secondary electrons generated by the beam as it bombarded the collector. The currents measured in this way agree well with the Child-Langmuir current within our present experimental error of

10% over a wide range of operating voltages up to the design voltage of 500 kV (Fig. 4). A pulsed Cs vapor source is required to supply enough Cs atoms to achieve space charge limited operation for voltages above 400 kV. A novel way of generating a pulsed cesium vapor source by vacuum spark has been tested and is being installed in the source chamber.

A radially scanning probe is used to measure the beam uniformity in the transverse direction. Our preliminary results show that the beam is approximately 90% uniform over the 30 cm beam diameter with less than 1 cm wide edges where the beam current drops rapidly to zero.

Potassium bromide (KBr) was found to be a suitable scintillating material for Cs^{+1} , emitting bright light which is visible with the naked eye even in the presence of the ambient light from the red-hot Ir plate. This technique is very useful in measuring the beam uniformity, and in giving an estimate of the beam emittance.

References

1. A. Faltens and D. Keefe, Proceedings of the Heavy Ion Fusion Workshop, Brookhaven National Laboratory, Upton, New York, October 17-21, 1977, BNL-Report 50769, p. 27.
2. W. Chupp, A. Faltens, W.B. Herrmannsfeldt, D. Keefe, S. Abbott, and E. Hoyer, *ibid.*, p. 88.
3. J.B. Taylor, and I. Langmuir, *Phys. Rev.* **44**, 423 (1933).
4. M. Hashmi and A.J. Van der Houven van Oordt, Conference on Isotope Separation, London, March 5-7 (1975).

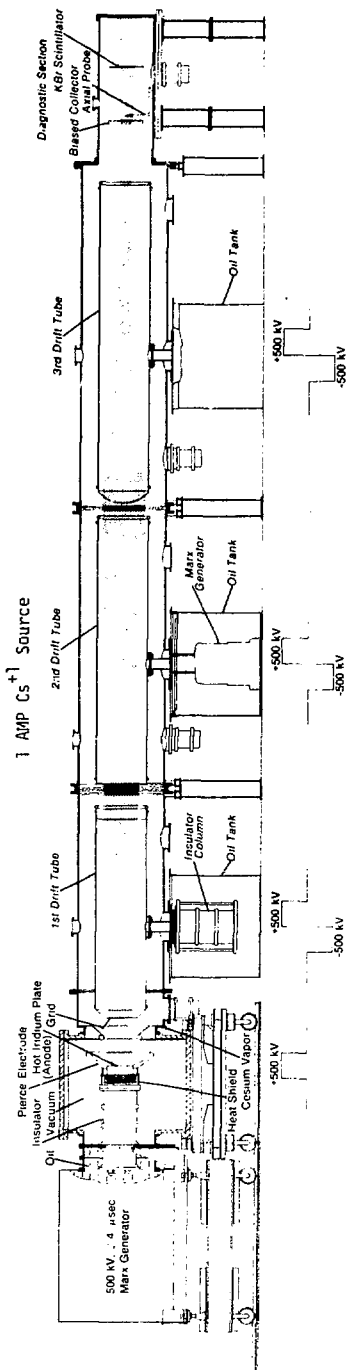


FIG. 1 - SCHEMATIC DIAGRAM OF THE EXPERIMENTAL APPARATUS.



FIG. 2 - TYPICAL VOLTAGE AND CURRENT WAVE FORMS.

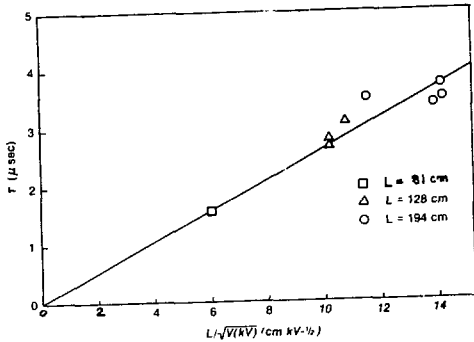


FIG. 3 - TIME OF FLIGHT MEASUREMENTS OF Cs^+ BEAM. L IS THE DISTANCE OF THE DRIFT SPACE.

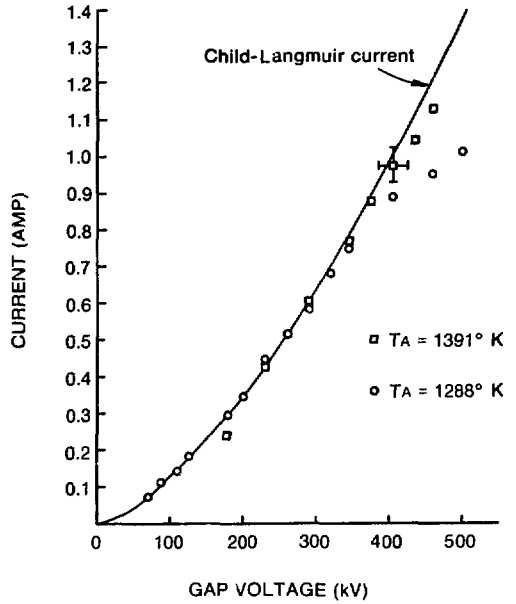


FIG. 4 - CURRENT VS. VOLTAGE APPLIED TO THE ANODE FOR TWO VALUES OF Cs EMISSION.

APPENDIX B

DESIGN/COST STUDY OF AN INDUCTION LINAC FOR HEAVY IONS FOR PELLET-FUSION*

Andris Faltens, Egon Hoyer, Denis Keefe, L. Jackson Laslett**

Introduction and Background

For electrons, the induction linac has been well-established as a high-current (≈ 1 kA) accelerator with high repetition rate, good electrical efficiency and high operational reliability.¹ In such systems the electrons are injected at relativistic speed so that the beam current, I , and pulse duration τ , remain constant along the accelerator. The design procedure thus becomes one of designing a single accelerating module (appropriate to the chosen I and τ) and iterating such modules until the final beam particle energy has been reached.

For a non-relativistic ($\beta < 0.5$) heavy ion induction-linac driver, however, the design procedure is much less transparent. For instance, the particle mass and charge can have a range of values - also the final beam voltage, V_f , (kinetic energy/charge-state, q), is a matter of choice since only the product, $I\tau V_f = Q$, is specified for a driver delivering Q joules. An important degree of freedom is available in such a machine - namely, the ability to achieve pulse compression by modest differential acceleration (slightly-ramped voltage pulses); this comes at the price - to the designer - of allowing a free choice of beam current over a wide range at any point along the machine. The upper bound on current is set by the transverse space charge limit; on the lower side, while there is no physical bound, in general one finds that a decrease in current is accompanied by a decrease in electrical efficiency and an increase in cost.

* This work was supported by the Office of Inertial Fusion of the U.S. Dept. of Energy under Contract No. W-7405-ENG-48.

**Lawrence Berkeley Laboratory, Berkeley, Calif. 94720

The physics of the pellet implosion sets stringent conditions on the accelerator driver. The beam energy should be > 1 MJ, the beam power > 100 TW (implying a pulse length ≈ 10 ns), and the specific energy deposition in the pellet > 20 MJ/g.

Thus, considerable current amplification is required, e.g. from some 10 amps at the source to perhaps 10 kiloamps at the pellet. Most of this amplification can be accomplished continuously along the accelerator and the remainder achieved at the end by bunching in the final transport lines to the target chamber.

Design Approach

A conceptual schematic of an Induction Linac Fusion Driver is shown in Figure 1, which includes an injector, an accelerator-buncher, and a final transport system. Here only the accelerator portion of the driver is discussed.

The essence of the design approach is to pick a specified total beam charge $[I\tau]$, one value in a sequence, and examine the differential cost, ΔC , required to add an increment of voltage $\Delta V = 1$ MV to the beam at each voltage point, V , along the accelerator. In general, there is a minimum value of $\Delta C/\Delta V$ at each voltage point, V , which in turn determines the exact design for the accelerating modules, pulsers and magnets at that point; if one seeks for example, a minimum-cost accelerator, the entire design is determined and the cost -- except for the injector and final beam manipulation sections -- is given by

$$[C_{\min}]_{[I\tau]} = \left[V_{\text{inj}} \int \left(\frac{\Delta C}{\Delta V} \right)_{\min} dV \right]_{[I\tau]}$$

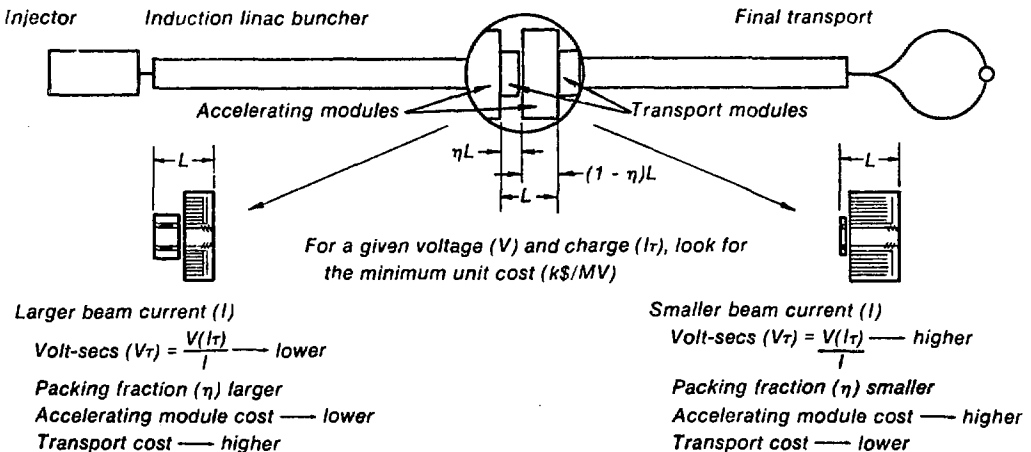


FIG. 1 - INDUCTION LINAC FUSION DRIVER

Some departure from the minimum-cost design, particularly at the higher voltage points, is probably desirable for electrical efficiency reasons and for meeting the final longitudinal space charge requirements. Thus it is important to have detailed information concerning the nature of the $\Delta C/\Delta V$ variation, i.e., whether it is a broad or narrow stationary minimum or if it is a non-stationary minimum arising from a constraint. See Fig. 3 for an example of a $\Delta C/\Delta V$ curve.

Methodology

We have simplified the problem in studying drivers by assuming:

- (i) A suitable injector at $V_{inj} = 50$ MV is available.
- (ii) The final rapid-buncher section costs about the same as if it were composed of a pure accelerating section with modest bunching.

To address the main part of the system, viz. Induction Linac, a computer program (LIACEP) has been developed to sort through the possible engineering options at each voltage point, V , along the machine and to generate the desired cost and design information. In Figure 2 a simplified flow chart of the LIACEP Program is shown.

We start by specifying an ion species with atomic weight, A , charge state, q , transverse emittance, ϵ_N , Detatron tune shift, Δv , and rep. rate f . Next, an electrical beam charge [IT] is specified with a sequence to be explored -- 30 μC , 60 μC , 90 μC ..., etc. Then at any voltage point, V , along the accelerator the cost consequences of adding further 1 MV are examined. The independent variable is chosen to be the current, I , with the magnet occupancy factor, η , for a symmetrical FODO lattice, as a separately set and varied parameter (e.g., $\eta = .5, .33, .17, .10, .05$, etc.). In this way a set of curves for each value of η can be generated to display differential cost versus current and so to arrive at a minimum or indicate the cost/benefit

ratio of departing from the minimum as shown in Fig. 3.

Key ingredients of the optimization process include: (1) Engineering design options and constraints, (2) Cost data base which can affect the trade-off among design choices, (3) Physics assumptions about (i) the desirable beam emittance determined by the pellet and transport requirements, or the realizable beam emittance set by the source performance, and; (ii) the transverse space charge limiting current.

The program cycles through three design configurations, see Figure 2, and consider four different core materials: ferrite, low carbon steel, nickel steel, and amorphous iron. Superconducting transport elements are considered. Cost data information is given in Reference 2.

The sensitivity of cost efficiency to the space-charge limited current seems a general feature and it becomes important to have a good understanding of what betatron tune depression can be safely tolerated in the transport system. Extensive studies of this question have been carried out by Laslett using computational techniques for a Kapchinskij-Vladimirskij distribution³ and by Haber using numerical simulation codes.⁴ At present a tune depression of $60^\circ - 24^\circ$ is used for a K-V distribution (60° with no current down to 24° at maximum current).

Example 1 MJ Driver

Results from the LIACEP program are shown in Figures 3 through 6 for a 1 MJ Driver with the following set conditions:

$$U^{+4} \quad \epsilon_N = 3.0 \times 10^{-5} \text{ meter radians}$$

$$I_T = 210 \mu C \quad \Delta v = 60^\circ - 24^\circ$$

$$f = 1 \text{ Hz}$$

Unit costs versus current for various packing fractions at a fixed beam voltage V are shown in Figure 3. Adopting the minimum cost options at

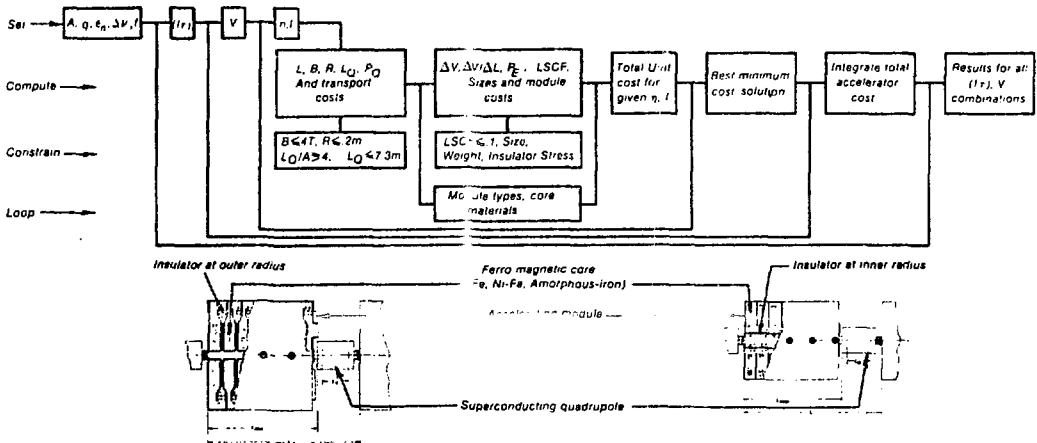


FIG. 2 - PROGRAM LIACEP FLOW CHART

various beam voltages, the minimum unit cost curve in Figure 4 is obtained. Integrating the unit cost curve with voltage yields the minimum accelerator cost also shown in Figure 4. Figures 5 and 6 show various accelerator parameters, namely, current, pulse duration, transport magnet field, and radius, for the minimum cost accelerator.

It must be emphasized that these cost studies are useful as a design guide and as a tool for identifying the cost sensitivity to any of the input assumptions and engineering options and costs. Thus the absolute value of the cost figures should be treated with considerable caution and attention focussed on the trends suggested by the data; reliable costs can be derived only when a particular case is settled upon and an ab initio design carried

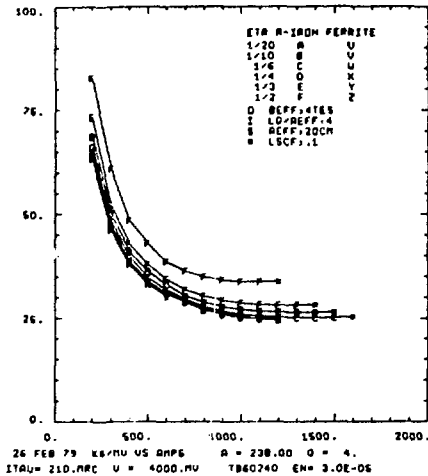


FIG. 3 - EXAMPLE COST CURVE

through in detail for that case.

We wish to acknowledge the help of Mr. Victor Brady in performing much of the computational work.

References

1. D. Eccleshall and J.K. Temperly, J.A.P. 49, July, 1978 for extensive references.
2. E. Hoyer, LBL, Eng. Note M5250, (1978).
3. L.J. Laslett, L. Smith, J. Bisognano, LBL Note: HI-FAN-43, (1978).
4. I. Haber and A. Maschke, NRL-3787, (1978).

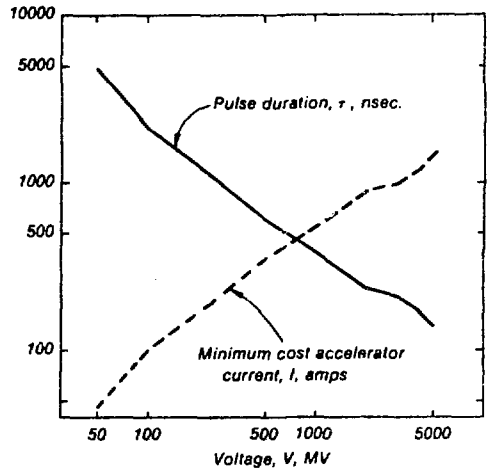


FIG. 5 - ACCELERATOR CURRENT AND PULSE DURATION

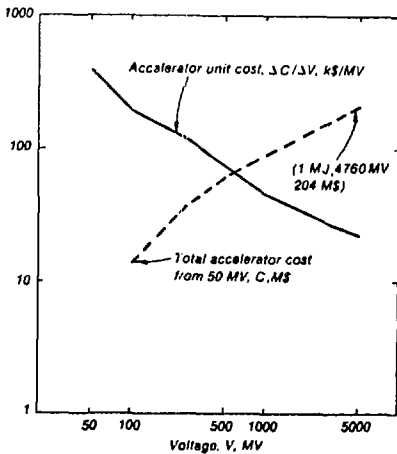


FIG. 4 - MINIMUM UNIT COST AND ACCELERATOR COST

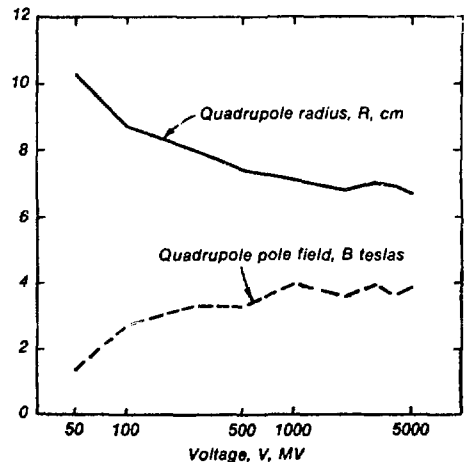


FIG. 6 - TRANSPORT MAGNET FIELD AND RADIUS

APPENDIX C

OPERATION OF A HIGH-CURRENT XENON SOURCE*

Warren Chupp, Dave Clark, Robert Richter, John Staples, and Emery Zajec**

Introduction

The development of heavy ion accelerator driver systems for inertial confinement fusion will also require the development of high current heavy ion sources. High current plasma arc sources have already been developed at LBL in connection with the neutral beam program.¹ This paper reports the results of adapting the Ehlers type source to produce singly charged Xenon ions and subsequently accelerate them to 500 kilovolts.

Summary

A multi-aperture Ehlers-type source has been constructed and operated to produce a 60 mA Xe^{+1} beam. The multi-aperture source utilizes a 13 hole aperture in a circular pattern producing a beam 25 mm in diameter. An "accel-decel" extraction system was used, producing a 22.5 keV beam whose normalized emittance at 29 mA was 0.027π cm-mrad. The neutralized beam was transported one meter through two magnetic quadrupole triplets to the entrance of a 20 cm accelerating gap consisting of five intermediate electrodes with a total voltage drop of 500 kV. The vacuum in the extraction region was held to 10^{-5} Torr by using a puff valve and two 1500 l/sec turbo pumps. Multi-wire profile monitors just ahead of the column entrance measured the beam size, which was in good agreement with single-particle transport calculations.

Ion Source Geometry

A schematic of the multi-aperture xenon source is shown in Figure 1. The electron current is supplied by a circular array of 8 .02" dia. tungsten filaments connected in parallel. The large hemispherical anode is shaped to reduce the arc potential, favoring Xe^{+1} production. The extraction lens is a 13 hole accel-decel system with typical operation voltages of 25 and 3 kV. Figure 2 illustrates the three hexagonal multi-aperture electrodes, the support insulators, and the source body in the order of assembly.

The filament and anode structure of the source was developed from an early model used in the LBL neutral beam project under W. Kunkel. This model was kindly lent to us by K. Berkner.

Low Voltage Test Stand Facility

The low voltage test stand consists of four principle components: the xenon source including its accel-decel lens, the pumping system, a 4 inch quadrupole triplet, and a 90 degree analyzing magnet. Two Sargent-Welch turbomolecular pumps provide a pumping speed of 3000 l/sec at the ion source, while a diffusion pump and an additional turbomolecular pump provide 1650 l/sec pumping in the transport system.

*This work was supported by the Inertial Fusion Department of the U.S. Department of Energy under contract No. W-7405-ENG-48

**Lawrence Berkeley Laboratory
1 Cyclotron Road
Berkeley, Calif. 94720

Diagnostic equipment includes several Faraday cups, a 32-wire X-Y beam profile monitor, a slotted plate emittance measuring device, and two sets of X-Y jaws to determine the beam size. Extraction and decel lens potentials are supplied by two unregulated supplies capable of delivering 80 kV at 10 mA dc with additional capacity to compensate for beam loading effects. The arc supply can deliver 300 volts at 50 amperes with a pulse length of 500 μ sec, and the paralleled source filaments are powered by a 10 volt 150 ampere dc supply. Pulsed gas is supplied to the source by a voltage-controlled piezo-electric valve.

The plasma density in the ion source was measured by inserting a Langmuir probe through the arc chamber perpendicular to the beam axis. The uniformity is within $\pm 1.5\%$ over the area of the 13 hole extraction area. Typical values of plasma density vary between 35 to 100 mA/cm² for a filament current of 136 amperes.

Most of the development work with the low voltage test stand was aimed at obtaining maximum beam current at the Faraday cup 1.3 meters from the source. A collimator was usually used in front of the cup, set to simulate the 1" dia. entrance aperture of the accelerating column of the high-voltage test stand. The geometric (unnormalized) acceptance area of this system is 90π cm-mrad horizontally and 34π cm-mrad vertically when the collimator full widths are 1 inch square. With this collimation 35 mA of Xe^{+1} was measured in the cup.

It was found important to use a transverse magnetic bias of a few hundred gauss on the cup to eliminate the effects of stray electrons from various sources. With only electrostatic bias of the collector or an electrostatic suppression ring, the current collected varied continuously with positive or negative bias voltage, indicating that a plasma existed in the beam pipe. The current measured in a beam transformer just after the source was up to 60 mA, but this includes electron current moving in the plasma column toward the source and was not used in the data analysis.

Calculations of beam optics with space charge included showed that even 1 mA of uncompensated space charge would cause a factor of 2 loss in transmission, so the 35 mA beam in the cup was at least 97% neutralized. The fact that the experimental settings of the quadrupoles were within 15-20% of those calculated without space charge indicated that the space charge is well compensated.

The neutralization is due to secondary electrons from beam hitting the pipe and collimators, and from beam ionization of the residual gas (mostly xenon near the source). This latter process occurs in roughly 300 μ sec, for 20 keV ions in a gas pressure of 10^{-5} Torr and an ionization cross section of $3 \cdot 10^{-16}$ cm². The observed rise time of the beam pulse at the cup is 30 μ sec, indicating a large contribution of the fast wall electrons to neutralization. The transport loss to the charge exchange $Xe^{+1} + Xe^0 \rightarrow Xe^0 + Xe^{+1}$ is estimated to be about 9%.

Analysis of Low Voltage Test Stand

The emittance of the Xe^{+1} beam from the source was inferred from a two-slit interception technique. With a Faraday cup measuring the total beam current, a two-jaw aperture is closed down upon the beam until a reduction in intensity is detected. Then a second aperture between the first aperture and the Faraday cup is closed down until it just intercepts the beam. To calculate the emittance in the active plane of the jaws, either the beam size at a third point or the position of the beam waist must also be known. The position of the waist from previous beam dynamics calculations is known to be within ± 10 cm of the first aperture. A calculation of the emittance with the waist anywhere in this region results in only a 10% uncertainty in the calculated value of the emittance, which is considered adequate accuracy.

Measurements of the Xe^{+1} beam size with two slits .81 m apart gave a beam radius of 1.08 and 3.81 cm. The unnormalized emittance area calculated from these data with the waist within ± 10 cm of the first slit is $\pi\epsilon_V = 45 \pm 10\%$ cm-mrad. For a total acceleration voltage of 22.5 kV, this corresponds to a normalized emittance area $\epsilon_N = .027\pi \pm 10\%$ cm-mrad. Approximately 5% of the beam was intercepted on the slits, so this emittance area corresponds to the 95% contour. The current within this contour is 29 mA.

High Voltage Test Stand Facility

After initial tests on the xenon source were completed in the low voltage facility, the xenon source was installed in a 500 kV test terminal. A schematic drawing of the terminal, transport and diagnostic systems is shown in Figure 3. Primary power for the dc filament supply, the four pulsed quadrupole supplies, the two turbomolecular pump supplies and other equipment is supplied by a 15 kW 400 Hz and a 5 kW 60 Hz alternator.

A 32 wire X-Y beam profile monitor is located at the entrance of the accelerating column to aid in the tuning of the pulsed quadrupoles. The beam current is monitored by a Faraday cup immediately following the source in the pumping manifold and by a 1-1/2" dia. Faraday cup near the exit of the accelerating column which is movable along the inside of the beam pipe from the column exit to some distance downstream. This cup was removed when the 30° analysis system shown in Figure 3 was used and replaced by cups near the entrance and exit of the analyzing magnet. Two quadrupole singlets upstream of the 30° analyzing magnet focus the beam.

Analysis of 500 keV Xe^{+1} Test Data

The emittance of the 500 keV Xe^{+1} beam was inferred from measurements of the transmission of the beam through a 3/4" diameter aperture followed downstream by a 1-1/2" diameter aperture, each at several longitudinal positions in the 500 keV beam. This technique is somewhat sensitive to the current density profile, which is not known in detail. Using fitting procedure, assuming the current density profile to be either uniform or parabolic, results in a 13% uncertainty in the calculated emittance, considered to be of satisfactory accuracy.

For a typical run, with the 3/4" aperture 21.0 cm from the last electrode in the 500 kV accelerating column, the current through the 1-1/2" aperture is measured from 14 to 35 mA with the larger aperture 61 to 15.2 cm downstream of the smaller aperture. The 3/4" aperture is positioned so that it is just start-

ing to intercept the beam. For a uniform (parabolic) distribution, the waist is calculated to be 15 (11) cm upstream of the small aperture and the unnormalized emittance area of the transmitted beam to be 30π (40π) cm-mrad, corresponding to a normalized emittance area of $.084\pi$ ($.11\pi$) cm-mrad at 500 keV. The transmitted beam current was 35 mA in this run. Currents of up to 60 mA have been produced, but the emittance at these higher currents has not been measured.

The 500 keV 35 mA beam was also magnetically analyzed by a magnetic spectrometer which deflected the beam through 30°. The Xe^{+1} charge state was found to be 90% of the total when operating at an arc voltage of 20 V. As is to be expected, higher arc voltages lower the Xe^{+1} percentage through the production of higher charge states. A complete charge state analysis has not been done at this time although it would be of interest to explore the production of higher charge states under different operating conditions.

References

1. W. R. Baker, et.al, Proceedings of the Symposium on Ion Sources and Formation of Ion Beams, BNL Conf. Report, 1971.

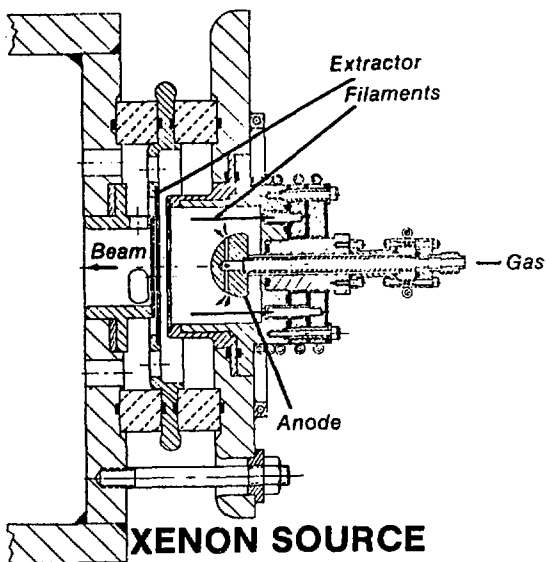
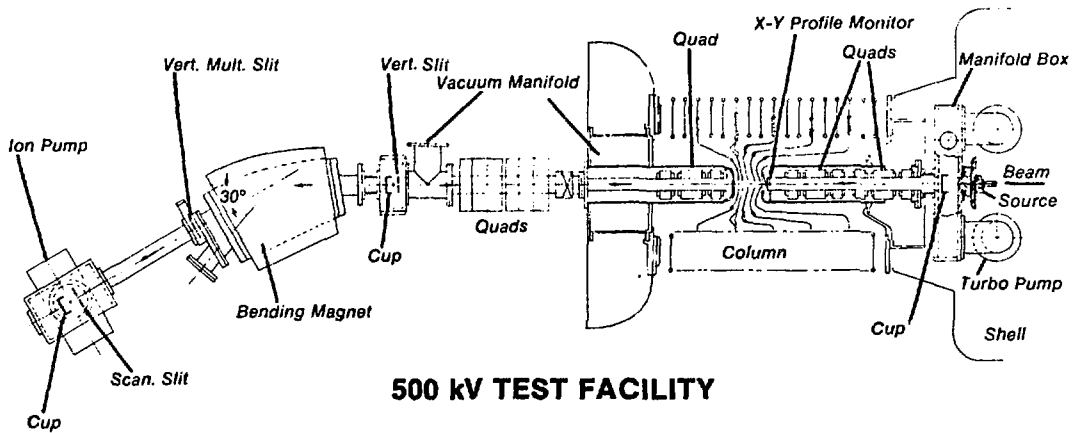


FIGURE 1



XBB 788-9617

FIGURE 2 - XENON SOURCE DISASSEMBLED



LBL 793-8706

FIGURE 3

APPENDIX D

A WIDERÖE-BASED HEAVY ION PREACCELERATOR FOR THE SUPERHILAC*

John W. Staples, Henry D. Lancaster and Roland B. Yourd**

Abstract

A new high-mass, high intensity injector for the SuperHILAC has been approved and is under construction at LBL. A high power intermediate charge state ion source and accompanying low-velocity linac will provide beams for subsequent acceleration by the SuperHILAC. Both axially and radially extracted ion sources will be accommodated and charge state analyzed in the 750 kV, 100 kHz Cockcroft-Walton terminal. The LEBT will provide isotopic analysis to 1 part in 300. A 5m long, 23.4 MHz Wideröe linac, operating in the $\pi-3$ mode based on the GSI design accelerates typically a U^{5+} ion to 113 keV/a where it is stripped to U^{11+} by a perfluoropolyether vapor stripper and further accelerated by the SuperHILAC. The space charge limit of the system is several electrical mA which will be approached in the intermediate mass range.

I. Introduction

A low-velocity, high current Wideröe linear accelerator is under construction at LBL. This accelerator system, including a new ion source and pre-injector, will serve as an injector to the SuperHILAC, supplementing two presently operating injectors, increasing the mass range to uranium and increasing the flux for ion species higher than argon up.

As the basic parameters of this injector have been covered in a previous paper¹ we will emphasize the highlights of this design, particularly those items of novel or unique interest that have already been built and tested individually.

The basic parameters of the injector have remained essentially constant except for the selection of charge state of the design ion, uranium, and the selection of the maximum terminal potential of the Cockcroft-Walton preaccelerator. The design charge state has been adjusted downward to U^{5+} to provide a larger available flux of ions. This means that Ar^{1+} will also be available, allowing us to experiment with the effects of accelerating large currents through the machine, near its space charge limit of approximately 10 eMA. The preaccelerator voltage has been raised to 750 kV to accommodate the reduction in charge state of the accelerated ion.

The Wideröe linac increases the kinetic energy of the accelerated ion from 15.8 keV/amu to 113 keV/amu for injection into the first tank of the

*This work was supported by the High Energy & Nuclear Physics Division of the U.S. Department of Energy under contract No. W-7705-ENG-48

**Lawrence Berkeley Laboratory
1 Cyclotron Rd.
Berkeley, California 94720

1. J. Staples et. al, A Wideröe Pre-Accelerator for the SuperHILAC, 1976 Proton Linear Accelerator Conference, P. 81.

SuperHILAC. After the Wideröe, the beam is stripped in a Fomblin vapor stripper. The stripping efficiency into a single charge state has been measured at 11% for Pb, rising to 17% for Xe.

II. Preinjector System Summary

The preinjector consists of a 750 kV high-frequency Cockcroft-Walton stack containing two ion sources in the terminal. An axial source of the Ehlers type is provided for the noble gases and a sputter-arc radially extracted PIG for the metallic ions. 90 kVA of power is available in the terminal through a rotating shaft drive. A 150 hp., 1,800 rpm motor will be located in a pit in the floor beneath the terminal house and a vertical 10" OD by 0.5" wall filament wound epoxy tube drive shaft will transmit the power to two generators in the high voltage terminal: a 65 KVA 60 Hz unit and a 25 KVA 400 Hz unit. Cryogenic pumping will be used near the ion sources to recover rare and expensive source gases and to reduce the power and weight requirements. Terminal cooling will be by means of Freon-113 circulated from the ground end to high voltage through 2-1/2" diameter insulating plastic tubes (nylon or delrin) at a flow rate of 40 gpm.

The accelerating column will consist of three 30 cm long sections of commercially available titanium-ceramic modules in an atmosphere of SF₆. Uniform grading is used, and the current limit is 15 eMA at 750 kV. In the 60 cm space between the source analyzing magnet and the column entrance a series of magnetic quadrupoles focuses and matches the beam. The very short cell length reduces the maximum tune depression to less than 0.5. For the maximum uncompensated space charge.

The LEBT between the column exit and Wideröe entrance contains four sets of doublets, steering, a 90° analyzing magnet and one fundamental frequency buncher of the quarter-wave line type. For low to moderate current, the analyzer will provide an isotopic mass analysis of one part in 300, allowing us to use natural source material for all but the most intense beam requirements.

IIa. Axial Ion Source

For ions from gaseous source material, we will use an axially-extracted source similar to those developed at LBL by Ehlers² for neutral beam injection and reported on elsewhere in this conference³. We have accelerated 60 eMA of Xe^{1+} from a version of this source to 475 keV and in another series of runs have shown that we can expect about 10% of the total beam output to be Xe^{3+} . This source shows a noise modulation of 0 to 10%.

IIb. Cockcroft-Walton

The CW power supply will be a half-wave cascade voltage multiplier operating at about 90 kHz. A stack of 10 decks will be topped by the

2160 ft³ terminal house. This arrangement results in a very compact structure. The support structure will be four 14" O.D. vertical support columns of filament wound fiberglass-epoxy tubes 10.75 ft. long. Each deck of the CW consists of two 200 kV PIV silicon rectifier modules, two 100 kV .025 μfd capacitors and surge limiting resistors. Spark gaps protect the components from excessive voltage during surge conditions: Ten decks, each rated to 100 kV are stacked to a height of ten feet, and the maximum gradient along the components of the power supply is 11 kV/inch.

The 90 kHz power is generated by two 4CW25,000 tetrodes operating class C into a resonator supplying the bottom end of the CW stack. Two regulation loops are provided: a slow one through a generating voltmeter and a fast one through a capacitive pick-off on the wall of the preinjector house. The power supply will provide a 10 ma average current with a maximum ripple of 500 volts. The load induced droop at 10 ma is about 3 kV which will be corrected by the drive to the 90 kV supply. No bouncer as such is used. The response time of the fast feedback system and the high frequency of the CW excitation provide adequate correction response time.

A CW power supply essentially identical to this one was recently put into successful operation at the SuperHILAC and has provided satisfactory service.

III. Wideröe Accelerator

The principle requirement of the injector system accelerator is to accelerate U⁵⁺ from a kinetic energy of 15.8 to 113 keV/amu. The Wideröe accelerator operates at 23.4 MHz and has a π-3 π drift tube arrangement with magnetic focussing quadrupoles in the even (long) drift tubes. The 5 meter long coaxial structure is supported by three stub lines which also control the resonant frequency and voltage distribution in the 34 drift tube gaps.

The tank will be fabricated from 0.5 inch 10% copper clad mild steel plate by a rolling and welding operation. Sealing between the tank and the end walls will be by O-rings and copper r.f. gaskets. At full gradient, the gap voltage varies along the structure from 100 to 250 kV, with a total peak power dissipation of 75 kW.

IIIa RF Power Amplifier

We will use an Eimac 4CW100,000 running Class AB₂ in the final amplifier stage. This tube can deliver over 200 kW in this mode giving us ample reserve to supply resonator losses and an expected 20-40 kW of beam loading. Running at 30% duty factor, we will have ample plate dissipation even when supplying reactive power to the beam load. In normal operation we will run at reduced filament voltage to extend tube life. It has been our experience that with the filament voltage reduced to about 90% of its rated value we can expect over 50,000 hours (5-7 years) of life on these tubes.

2. W. R. Baker et al., Proceedings of the Symposium on Ion Sources and Formation of Ion Beams, BNL Conference Report, 1971

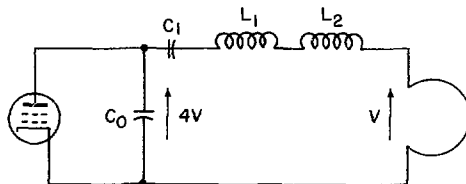
3. E. Zajec et al., Operation of a High-Current Xenon Source, Paper B-18, this conference.

As in the design used successfully at the SuperHILAC, the final amplifier will be tightly coupled to the accelerating structure using a loop in one of the stub lines. The voltage equation for the coupling loop is

$$j\omega LI_L + j\omega HA = V_L$$

The second term is the voltage induced in the loop by the cavity field. This voltage is in phase with the input voltage, V_L , and accounts for the real power transfer to the resonator. The first term represents the voltage drop due to loop self-inductance. When coupling to Alvarez type linac cavities at the SuperHILAC this term is reduced to zero by adding a capacitive reactance to tune in out.

In an Alvarez type linac cavity the magnetic field at the wall is high enough so a reasonable size loop will give an induced voltage adequate for matching to high power r.f. tubes, about 15 kV, so there is no need for a matching network between the tube plate circuit and coupling loop. For the Wideröe structure the field at the stub line wall is much lower, and the dimensions are smaller. A reasonable coupling loop size gives an induced voltage of about 4 kV. Because this voltage is so low a simple matching network will be added between the 4CW100,000 and the coupling loop to increase the voltage by a factor of four. This will be done by adding an inductance in series with the coupling loop and adjusting it in conjunction with the 4CW100,000 output capacity for the proper step-up ratio. Figure 1 shows the equivalent circuit matching the plate impedance to the drive loop.



XBL 793-736

Fig. 1

The final amplifier and its driver will be built into an enclosure that is mounted directly on the side of the stub line of the Wideröe. The final amplifier has no plate resonator as such, just a decoupling choke for the B+ supply line. The r.f. to the driver stage will be derived from a solid-state 10 watt amplifier module located remotely.

IIIb. Tape-Wound Drift Tube Quadrupoles

The sixteen long drift tubes in the accelerator contain magnetic quadrupoles arranged in four groups. The integrated gradient-length product for all of them is 97.5 kgauss with the clear aperture diameter increasing from 1.6 cm for the first five units to 3.0 cm for the last seven. The most difficult quadrupole is the first with an effective length of 7.84 cm and a gradient of 12.44 kG/cm. We have build and successfully tested two versions of this device.

The construction techniques for tape-wound magnets have been published previously⁴. In this application, the requirements of high gradient in a short effective length were met by using pole tips 7.16 cm long and tapered made of vanadium perandur, contained in a yoke whose outer diameter is 20 cm. The coil is wound with 28 turns of 0.5mm thick copper tape and the measured efficiency at full field is 85%, the electrical requirements being 13.6 volts at 169 amperes.

The drift tube surfaces and magnet coil are flood cooled by Freon TF-113 at a flow rate of 3-5 gpm. The drift tube is supported from below by a single stem (inverted configuration) and the coolant return is from an aperture at the top (opposite the stem) so a gas bubble will not form and be trapped. The total weight of the drift tube assembly is 20 kg.

Figure 2 shows the completed prototype quadrupole. Sensing loops are shown placed around the pole base, pole tip and return yoke to monitor flux in those regions as a function of excitation.

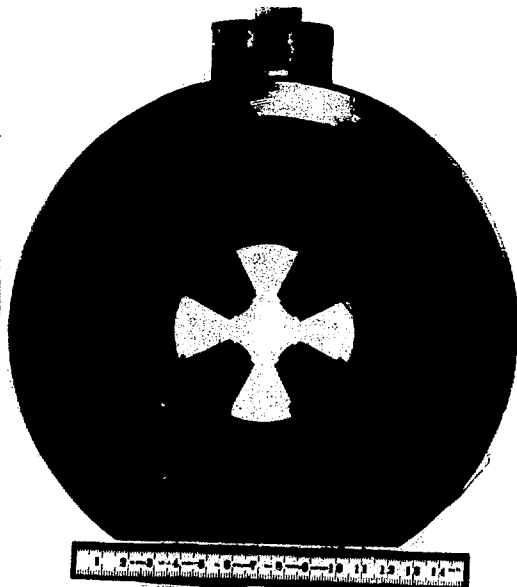


Fig. 2

IV. Matching, Stripping and Control

The beam is stripped immediately following the Wideröe and transported 12.5 meters to the entrance of the SuperHILAC. A vertical translation is included. At the SuperHILAC entrance, a fast switching magnet selects one of three possible injectors in any arbitrary 36 pulse per second sequence. The SuperHILAC itself and the beam switchyard presently have this fast beam multiplexing facility, providing at present two ion species. No debunching-rebunching will take place in the near future. Therefore about a 50% transfer efficiency of the selected charge state from the stripper to the SuperHILAC r.f. bucket is expected. When bucket matching is later introduced, the energy stability of the Wideröe

must be held to $2 \cdot 10^{-4}$.

IVa. Fluorocarbon Stripper

The stripper following the Wideröe raises the mean charge state of the beam so that acceleration can continue in the first tank of the SuperHILAC. The beam is analyzed in the transport line following the stripper to select the charge state required. The stripper material is a fluorocarbon vapor of high molecular weight at a pressure of about 1 Torr evaporated from a reservoir of liquid. This type of stripper imposes no limit on the beam power and is a low maintenance item. In addition, Fomblin cracks into lighter fragments in the presence of beam which are easily swept from the stripping area.

The vapor stripper will consist of a reservoir of Fomblin Y-Vac-25/9 liquid electrically heated to no more than 200°C by a resistance heater. At the top of the reservoir a water cooled surface thermally isolated from the reservoir will condense the vapor back into the heated bath.

The aperture diameter of the stripper is 1 cm. A cooled beam scraper will be located upstream of the stripper to protect it from missteered beam or halo.

The stripping characteristics of this material have recently been measured with the above desired stripper at LBL by Alonso and Leemann⁵ for Kr, Xe, Ho and Pb. The stripped beam shows a high asymmetry of the final charge state distribution, probably due to the long chainlike nature of the molecule. The mean charge state at a beam energy of 113 keV/amu lies between that for gas and solid strippers, but the skew toward the high charge states with Fomblin provides substantial fluxes of the charge states of interest. For a q/A of greater than .046, that needed by the SuperHILAC, 11.5% of Pb^{10+} is available, rising to 14.5% of Ho^{6+} , 17% of Xe^{9+} and 21% of Kr^{6+} , the percentages normalized by particle count. The corresponding numbers for a thin carbon foil stripper run between 17% to 25%. However, the equilibrium thickness for carbon is less than 1 μ g and the power limit is low. The small angle scattering in Fomblin is significantly lower than that for a foil stripper. Figure 3 shows these charge state distributions.

4. R. M. Main and Ron Yourd, Edge Cooled Tape Magnet Coils for High Current Density Application, Forth International Conference on Magnet Technology, BNL (1972)

5. J. R. Alonso and B. T. Leemann, Fluorocarbon Stripping of Low Heavy Ions, Paper D-4, this Conference.

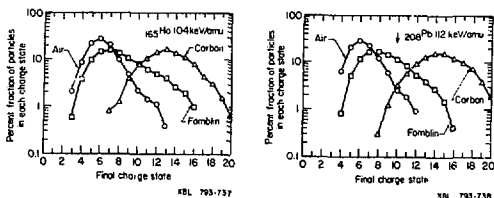


Fig. 3

APPENDIX E

POSSIBLE LOWER LIMIT TO LINAC EMITTANCE*

John W. Staples**
Robert A. Jameson***

Abstract

Numerical calculations made by several groups have always shown that an asymptotic lower exit emittance exists for linacs operating with high beam current as the input emittance is reduced to zero. In this paper, a mechanism for this limit is shown to be spread in the betatron frequencies of the individual particles due to the combination of space charge and r.f. gap forces, causing different transverse trajectories correlated with the instantaneous longitudinal position of the particle. These trajectories cannot all be simultaneously matched to the average restoring forces, resulting in an overall emittance increase if the space charge force is a large fraction of the restoring force. In principle, equilibrium distributions may exist which would not grow. Raising the linac frequency or reducing longitudinal emittance improves the situation, but higher injection energy does not.

Introduction

Chasman¹ showed in 1968, using a particle tracing code, that the normalized output emittance of a 10 MeV 200 MHz linac reached an asymptotic lower limit as the input emittance was reduced to zero. She also showed that this limit decreased with beam intensity and that the longitudinal-transverse coupling due to the r.f. fields alone was not responsible for this lower emittance limit. More recently, Jameson and Mills² conducted a parameter search, also with a particle tracing program (PARMLA), confirming Chasman's result and further showing the surprising result that this lower limit is substantially independent of the injection energy but is directly correlated with operating wavelength, and to a lesser extent, synchronous phase and accelerating gradient. This result was analytically confirmed by Lysenko³, working from an equilibrium distribution analysis. This paper offers an explanation of these phenomena.

Recent Observations

Several groups, primarily at LBL and LASL, have been investigating this blow-up phenomenon for heavy ion fusion and other applications. These groups observed several consistent phenomena:

- (a) There is a lower limit to the output emittance of a linac (Fig. 1)
- (b) The growth in emittance is initially very rapid -- in the first 2 or 3 cells
- (c) There is a slow subsequent growth
- (d) The r.f. longitudinal-transverse coupling without space charge is not responsible for the majority of this growth
- (e) The growth is almost independent of injection energy over reasonable limits
- (f) Reducing the longitudinal emittance helps
- (g) There is a strong positive correlation of emittance limit with operating wavelength
- (h) The effect is not strongly dependent on the initial particle distribution (KV or non-KV) with the same rms properties

In tracking up to 1000 particles it is observed that the periphery of the transverse phase space quickly becomes filamented and that the lobes are correlated with the instantaneous longitudinal position of the particle. Furthermore, upon tracing orbits of individual particles, it is seen that particles near ψ_s have a strong transverse tune depression due to space charge forces and particles near the ends of the bunch have lesser transverse space charge effects but are differentiated by stronger or weaker r.f. defocusing. Figure 2 shows the filamented phase space at the second cell of a typical linac, along with the transverse phase space for five longitudinal slices, each 10 degrees wide. The normalized transverse emittance here has almost doubled from the initial value of .05 π cm-mrad.

Matching

The average beam can be matched in the "smooth" sense if no envelope oscillations occur over the strong focussing flutter. If \bar{a} and \bar{c} represent the averaged matched transverse and longitudinal beam radii in a linearized approximation, then in an Alvarez structure operating in the $\beta\lambda$ mode

$$\left(\frac{\Delta u}{2}\right)^2 - \left(\frac{\epsilon_L^0 \lambda}{\bar{a}}\right)^2 = 90\Omega \left(\frac{e}{mc^2}\right) \frac{I \lambda^3}{2\beta^2 \bar{c}} (1-f') \quad (1)$$

$$-2\pi \left(\frac{e}{mc^2}\right) \frac{E_0 T \sin \phi_s \pi}{\beta} - \frac{(\epsilon_L^0)^2 \lambda^3}{(2\pi mc^2)^2 \bar{c}^2} = 90\Omega \left(\frac{e}{mc^2}\right) \frac{I \lambda^2 f'}{\bar{a}} \quad (2)$$

where ϵ_L^0 is the initial longitudinal emittance area in radian-eV, ϵ_T^0 is the initial normalized transverse emittance area, $f = \bar{a}/(\bar{a}+2\bar{c})$ is a geometric form factor, I is the average beam current, and Δu is the transverse phase advance per quadrupole cell without space charge. Figure 3 shows the matched transverse beam radius in the smooth approximation as a function of emittance for various frequencies, currents and injection velocities. This method gives a fairly good approximation to a matched beam, defined as an absence of envelope oscillations. Small adjustments to the parameters are made to eliminate any residual mismatch. As the initial transverse emittance decreases the beam size approaches a constant,

*This work was supported by the High Energy & Nuclear Physics Division of the U.S. Department of Energy under contract No. W-7405-ENG-48

**Lawrence Berkeley Laboratory
1 Cyclotron Rd.
Berkeley, California 94720

***Los Alamos Scientific Laboratory
P.O. Box 1663
Los Alamos, New Mexico 87545

dependent upon the transported current, and the maximum angular divergence decreases in direct proportion to the emittance. These beams are "delicate" -- a small non-linearity can cause large relative changes to the divergence, increasing the area of its trajectory. An even more important mechanism, is the strong effect the varying balance of restoring forces at various values of ϕ have on the axis ratio (x/x') of the trajectories. This indicates that in the presence of space charge, a particle's transverse trajectory is highly correlated with its longitudinal position and that a simultaneous match for all particles does not exist, at least for the mathematical distributions we usually test, which are often uncorrelated or only constrained to be within multi-dimensional hyperellipsoids. Work presently in progress⁵ is exploring the existence of truly matched beams in accelerator systems. Present real beams appear not to be matched in this sense and therefore the hypotheses are useful. The lower emittance asymptote of a linac can be estimated to be near the region where the beam size begins to be independent of the beam emittance.

Reducing the Emittance Asymptote

If transverse emittance, \bar{a} and \bar{c} are scaled with λ , and E_0 inversely, Equations (1) and (2) remain invariant for constant I and $\Delta\mu$. This implies that the asymptotic emittance scales directly with wavelength if the accelerating and focussing gradients are scaled correctly. The transverse tune depression of a beam of a given current in a periodic focusing lattice decreases with decreasing cell length of the lattice. The velocity dependence in Equations (1) and (2) is weak, explaining the relative insensitivity to injection energy. Reduction in longitudinal emittance tends to reduce the phase spread slightly, thereby reducing the range of r.f. defocussing. This reduces the transverse emittance growth, but the effect is not large. Other matching procedures which account for the particular input distribution and the complete nature of the accelerator are now being studied, and we also hope to be able to better simulate actual beams.⁶ These procedures also allow matching to a point further along the accelerator when the emittance has stabilized. However, it is also possible that only the growth rate for non-equilibrium distributions will be affected.

Technological Implementation

Reductions in emittance growth would be achieved most successfully if we were able to prepare distributions for injection into the accelerating system which were in six-dimensional equilibrium with it. A new low- β accelerator structure may make this possible to a degree not previously achieved in linear accelerators. This structure, invented in the USSR, is under development at LASL^{7,8} and is named the "space-uniform-focusing" or "rf quadrupole" structure in which a beam can be taken from the ion-source/injector system at very low energy (≤ 100 keV), and adiabatically subjected to transverse strong focusing. At a few MeV, a bunch well fitted to the strong-focusing accelerating

system is formed, and a smooth transition is made into an Alvarez structure. Strong transverse focusing is achievable in the space-uniform-focusing structure; the practical limits for this type of structure are now under intensive investigation at LASL.

Exploiting higher operating frequencies for better control of transverse emittance brings attendant problems, because stronger focusing forces are required and tolerances become tighter. Recent technological advances have significantly extended the range of feasibility. Tests⁹ on a 6 cell, $\beta = 0.3$, 440 MHz Alvarez structure achieved 8 MV/m field gradients.

Very strong quadrupole focusing, on the order of 50 kG/cm for apertures of a few millimeters, are possible using rare-earth cobalt permanent magnets using the techniques of Halbach.¹⁰ Studies and tests of such quadrupoles, including tolerance requirements, are in progress at LASL. These gradients are appropriate for 100mA of protons at 440 MHz.

Finally, it is conceivable that transverse focusing for even higher frequency accelerators could be provided by inserting a longitudinal accelerating structure into a superconducting solenoid.

It is clear that the successful combination of these technologies and an increased understanding of emittance growth will find many applications, including, for example, heavy-ion fusion, precision radiography, and high-quality high-intensity beams for experimental physics and chemistry.

References

1. R. Chasman, 1968 Proton Linear Accelerator Conference, BNL 50120, p. 372
2. R. A. Jameson & R. S. Mills, "Factors Affecting High-Current, Bright Linac Beams," April 8, 1977, LASL, private communication.
3. W. Lysenko, "Equilibrium Phase-Space Distributions and Space Charge Limits in Linacs," LA07010-MS, October 1977, Los Alamos Scientific Laboratory.
4. Lloyd Smith, HIFAN-13, LBL, Oct. 4, 1977.
5. W. Lysenko, "Linac Particle Tracing Simulations," 1979 Particle Accelerator Conf. (these proceedings).
6. O. R. Sander & R. A. Jameson, "Recent Improvements in Beam Diagnostic Instrumentation," 1979 Particle Accelerator Conf. (these proceedings).
7. J. M. Potter, R. H. Stokes, et al, "RF Quadrupole Beam Dynamics," 1979 Particle Accelerator Conf. (these proceedings).
8. R. H. Stokes, K. R. Crandall, et al, "RF Quadrupole Beam Dynamics," 1979 Particle Accelerator Conf. (these proceedings).
9. D. A. Swenson (Comp), "Semiannual progress report for the PIGMI program at LASL," Jan. 1, June. 30, 1978, Los Alamos Scientific Laboratory.
10. K. Halbach, "Strong Rare Earth Cobalt Quadrupoles," 1979 Particle Accelerator Conf. (these proceedings).

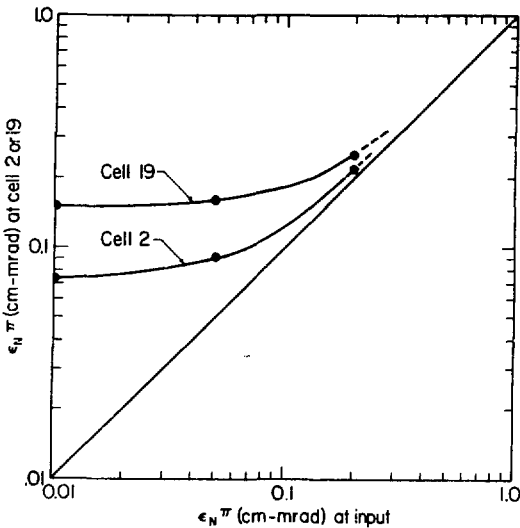


Fig. 1 Normalized transverse exit emittance as a function of entrance emittance in a 200 MHz linac carrying 100 mA of current. The injection energy is 750 keV and the beam is matched transversely and longitudinally.

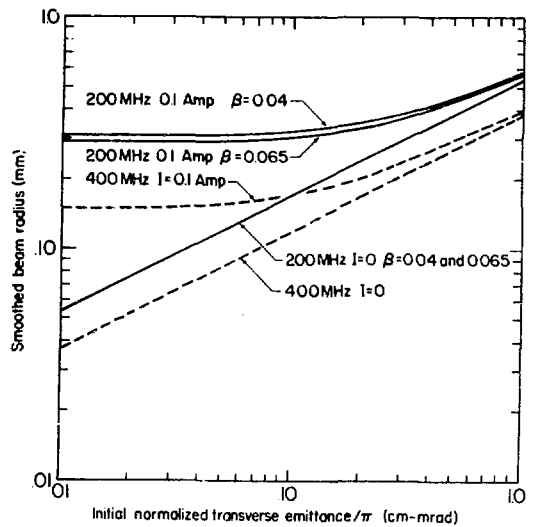


Fig. 3 Matched smoothed beam size for 200 and 400 MHz linacs carrying 100mA. The corresponding zero-current matched beam sizes are also shown; the phase advance per period is 60° . The injection velocity β is .04 in all cases, and also .065 in the case of the 200 MHz linac. The average axial field is 2.0 MV/m at 200 MHz and 3.3 MV/m at 400 MHz.

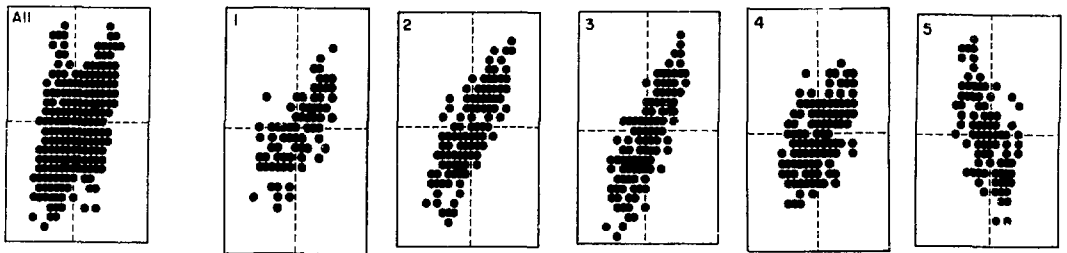


Fig. 2 Transverse yy' phase space at cell 2 of a 200 MHz linac injected at 750 keV. The first diagram shows the total phase space population. The next 5 diagrams show the yy' phase space for 10° longitudinal slices: diagram 1 for $\phi < -45^\circ$, 2 for $-45^\circ < \phi < -35^\circ$, 3 for $-35^\circ < \phi < -25^\circ$, 4 for $-25^\circ < \phi < -15^\circ$, and 5 for $-15^\circ < \phi$. The scales are ± 0.5 cm by ± 15 mm.

APPENDIX F

PROJECTS FOR HIGH ENERGY HEAVY ION ACCELERATORS*

Christoph Leemann**

Introduction

The acceleration of heavy ions to relativistic energies ($T \geq 1$ GeV/amu) at the beam intensities required for fundamental research falls clearly in the domain of synchrotrons. Up to date, such beams have been obtained from machines originally designed as proton accelerators by means of modified RF-programs, improved vacuum and, most importantly, altered or entirely new injector systems. Similarly, for the future, we do not foresee substantial changes in synchrotron design itself, but rather the judicious application and development of presently known principles and technologies and a choice of parameters optimized with respect to the peculiarities of heavy ions.

The low charge to mass ratio, q/A , of very heavy ions demands that superconducting magnets be considered in the interest of the highest energies for a given machine size. Injector brightness will continue to be of highest importance, and although space charge effects such as tune shifts will be increased by a factor q^2/A compared with protons, advances in linac current and brightness, rather than substantially higher energies are required to best utilize intensity wise a given synchrotron acceptance. However, high yields of fully stripped, very heavy ions demand energies of a few hundred MeV/amu, thus indicating the need for a booster synchrotron, although for entirely different reasons than in proton facilities. Finally, should we consider colliding beams, the high charge of heavy ions will impose severe current limitations and put high demands on system design with regard to such quantities as e.g., wall impedances or the ion induced gas desorption rate, and advanced concepts such as low β insertions with suppressed dispersion and very small crossing angles will be essential to the achievement of useful luminosities.

Present Status

Fig. 1 summarizes beam performance obtained or projected for the near future at presently operating facilities of which all except the CERN PS are or will be supporting a research program devoted predominantly or to a substantial degree to heavy ion research. Deuterons and α -particles of ~ 15 GeV/amu were obtained at the CPS, utilizing the (2β) -mode in the injector linac and a harmonic jump with intermediate flattop and adiabatic de/re-bunching in the synchrotron¹⁾. Deuterons were stacked in the ISR to a luminosity in excess of 10^{30} cm⁻²s⁻¹. Fully stripped ions from an EBIS-source and acceleration in the 2β -mode characterize the injector systems at both the synchrotron Saturne II²⁾. Light ion beam intensities comparable to those of Saturne are obtained at the Bevalac by accelerating partially stripped ions (e.g. C⁴⁺) from a PIG-source in the old 20 MeV proton linac, while for higher intensities and masses the Superhilac³⁾ serves as injector. These systems are limited by injector

performance and synchrotron vacuum. The sharp drop, e.g. in intensity between $A = 40$ and $A = 56$ observed at the Bevalac is predominantly due to the present vacuum of $2 \cdot 10^{-7}$ Torr. The presently ongoing Bevalac improvement program therefore includes first a new injector for the Superhilac, a Wideröe accepting a minimum q/A of 0.02 to provide intense high mass beams⁴⁾ and second, an improvement in synchrotron vacuum to 10^{-10} Torr⁵⁾ to assure survival of these beams in the Bevatron.

Future Facilities

Beam Requirements - Ideally we would base the design of new facilities on relatively firm specifications of basic parameters such as ion masses, beam intensity and energy, derived from experimental needs. The study of relativistic heavy ion collisions, although becoming respectable and recognized as a frontier in physics, is still a very young branch of science and although symposia and workshops (GSI, 1978, LBL 1979) will undoubtedly help to clarify design goals, it is unavoidable that at present our design efforts are based to a somewhat larger extent on speculative ideas than is the case e.g., for present major proton projects where a few big, simple issues can be pinpointed.

The trends are clear however, intense beams of the heaviest ions are required and smooth energy variability from ~ 100 MeV/amu up in the 10 to 20 GeV/amu range are desired. The need for ultra high energies is more speculative but the study of the implications of colliding beams seems indicated, if only in the interest of the longest useful life time of a major new facility.

Concepts for New Facilities

Approximate performance expectations of concepts developed in Japan, the USSR, Germany and the U.S. are summarized in Fig. 2. None of them represents a completely funded construction project but test facilities for the Numatron have been built, the Soviet proposals are expected to become reality within the next 5 years and funding for the GSI machine seems virtually assured. A formal proposal for the latter is just being worked out at present but the project has the advantage of an existing powerful heavy ion linac, and a substantial amount of R&D in the area of magnets, RF and vacuum systems conducted in the context of an earlier more modest proposal known as SIS⁶⁾. At LBL, where the Bevalac improvement program represents the present main commitment in the heavy ion field, preliminary studies have been conducted at a modest effort level exploring the feasibility and implications of a combined accelerator/storage ring facility^{7,8)}. Specialized heavy ion linacs are proposed throughout, linacs with low β front ends suitable for weakly charged ions, an interdigital H-mode structure in the Russian concepts, Wideröes in all others. At LBL and to some extent at GSI the linac itself is viewed as one of the main target areas for intensity improvement but other concepts are found. The Numatron⁹⁾ proposes an accumulator ring combining multiturn injection in betatron phase space with stacking in momentum space while stripping injection is an integral part of the Soviet concept and has, in modified form, been

*This work was supported by the High Energy & Nuclear Physics Division of the U.S. Department of Energy under contract No. W-7405-ENG-48

**Lawrence Berkeley Laboratory
Berkeley, California 94720

considered at GSI as well¹⁰). The Numatron approach will increase intensity from the synchrotron, although at the expense of increased longitudinal emittance, requiring substantial RF-voltage and precluding later stacking such as would be required in a colliding beam facility. Stripping injection at low energies (~10 MeV/amu) promises true brightness increase, somewhat analogous to stripping H⁻-injection known from proton synchrotrons¹¹), but only if all charge states occurring with significant probability after passage of the beam through a stripper are accepted. This requires a lattice with large momentum acceptance, strong sextupole correction to deal with chromaticity and zero dispersion at the stripper location to avoid the excitation of large betatron oscillations. Furthermore problems associated with energy loss and multiple scattering have to be overcome but the Soviet originators of the concept are confident that beam cannot only be accumulated in this fashion but actually accelerated, stripping to increasingly higher mean charge states until at energies between 200 and 300 MeV/amu transfer to the synchrotron, or in a more distant future, the Nuklotron would occur¹²).

None of these concepts proposes a rapid cycling main ring, conventional magnets will be used in the Numatron and the GSI machine, while superconducting magnets are foreseen for the Nuklotron and were assumed in our studies at LBL.

The LBL-Study as a Design Example

The LBL - study results will be used in the following to convey an idea of the looks of a potential major heavy ion facility and to illustrate some elementary design considerations.

Facility Layout and Operational Modes - Fig. 3 shows two rings with superconducting magnets injected by a heavy ion linac. Indicated is a B₀ of 80 Tm but presently we foresee 175 Tm, 5 T peak field and 1 T average field. Injection will occur without stripping at the linac exit in ring 1 while extraction is accomplished from ring 2. A number of transfer points between the two rings are indicated. With this arrangement 3 distinct modes of operation become immediately evident.

For energies not exceeding those achievable with partially stripped ions (9.6 GeV/amu for q/A = 0.2, B₀ = 175 Tm) ring 2 is not required for acceleration. The field in ring 1 can follow a simple triangular pulse shape with single turn ejection-injection transfer to ring 2 which serves then as a stretcher ring. Slow resonant extraction from ring 2 will then provide 100% duty cycle beam on target.

For higher energies stripping is required. Beam is accelerated in ring 1 to an energy sufficiently high to allow essentially lossless stripping in the fully ionized state. At this energy ejection, stripping and injection in ring 2 will occur where acceleration to the desired final energy, followed by slow extraction completes the cycle. Average flux on target may be increased by accommodating several pulses in ring 2, either stacking in longitudinal phase space or, if the required stripper thickness allows, by stripping injection.

Finally a colliding beam mode can be envisaged. To this end partially stripped ions are again accelerated in ring 1 (to full field), ejected, stripped and stacked in ring 2. Upon

completion of the stacking operation the field in ring 1 is reversed, the beam in ring 2 is bunched on a low, even harmonic and half the bunches are transferred to ring 1 by means of the S-shaped reinjection loop. Acceleration or deceleration to the desired operating energy followed by debunching then produces the desired final configuration: counter-rotating coasting colliding beams.

Rationale For This Approach

The basic consideration underlying this solution are outlined in the following and this concept will be seen to follow naturally from simple considerations even if at the outset we concentrate only on optimizing fixed target performance.

Superconducting Magnets - High field magnets are essential with the low value of Z/A of very heavy ions, especially if compounded by the inherently low packing factor of a colliding beam facility. They seem desirable however for an exclusive fixed target synchrotron as well. Undoubtedly R&D will be required but it is encouraging to note that recently at LBL¹³) an ESCAR type magnet with improved coil compression and helium circulation reached 4 T in continuously pulsed operation at 1 Ts⁻¹ and 3.77 T at 1.9 Ts⁻¹. The total power loss was 20 W for the 1 m long magnet at 1 Ts⁻¹ and improvements to reach 10 W only seem relatively straightforward. This translates into just over 1 MW input power to the cryogenic plant for one of our 175 Tm rings, quite favorable compared with ~ 20 MW power dissipation for conventional magnets assuming a gap of 70 mm and a current density of 1000A/cm². Net savings will be less than the factor of 20 implied but the potential for substantial economies cannot be denied.

Injector Considerations - Optimum utilization of synchrotron acceptance is achieved when we reach the space charge limit at injection, as given by the Laslett tune shift equation. From this, assuming a certain dilution $D_L = D_x D_z$ of transverse phase space density, a minimum linac brightness is calculated. In practice we want also to impose a limit on the number of injected turns which implies a condition on linac current. Fig. 4 summarizes for an ion with $A = 200$, $q/A = .2$, $.3$, $.4$ the required values, $B_L R$ and $I_L B_L R^2$, where B_L , I_L are linac brightness and current, R the synchrotron radius. Clearly higher energies are required to reach the same space charge limited synchrotron current for higher values of q/A (provided they were available at all). More importantly we see that with the assumed values ($\epsilon_{z,s} = \epsilon_{x,s} = 2 \cdot 10^{-4}$ m, $R = 175$ m $D_L = 10$) present linac performance indicates a severe brightness rather than space charge limitation and that even with values of 50 particle μA in $\pi \cdot 10^{-5}$ m, an ambitious but realistic long term goal for injector linacs, injection energies not much higher than ~ 10 MeV/amu are adequate.

It seems likely that $q/A = 0.2$ is the maximum we might expect from a bright, high current linac for very heavy ions without resorting to stripping at the linac exit. Consequently, the maximum energy obtainable with a given B₀ is substantially reduced compared to that for fully stripped ions. This is indicated in Fig. 5, where we however see that stripping at the linac exit with 10 MeV/amu $\leq T \leq 20$ MeV/amu will allow energies of between 80% to 90% of the maximum possible value. This is of course associated with a loss in intensity of about one

order of magnitude. Experimental data on stripping of very heavy ions at energies of hundreds of MeV/amu are not available, or possible to obtain, today and we have to rely on semi-quantitative theoretical considerations¹⁴, which indicate that 10% to 20% yields of fully stripped very heavy ions should be expected for 200 MeV/amu $\leq T \leq 300$ MeV/amu. A cautious guess is that ~ 1 GeV/amu is required to achieve essentially lossless stripping of very heavy ions in the completely ionized state. This requires a substantial booster. Only for main ring rigidities of 1500 Tm, i.e. approaching the size of the FNAL main ring is it possible to achieve a value of $B_{\text{booster}}/B_{\text{main ring}}$ comparable to that for typical proton facilities. In the presently more relevant range, 100 Tm $\leq B_{\text{MR}} \leq 200$ Tm, the booster will have a rigidity of $0.16 B_{\text{MR}} \leq B_{\text{BP}} \leq 0.35 B_{\text{MR}}$.

We see that the combination of an intense linac, 10 MeV/amu $\leq T \leq 20$ MeV/amu with a single, large ring will provide a quite powerful combination and a satisfactory first step towards a high performance fixed target facility. The ultimate in performance requires a booster of substantial size however, and from here it is only a small logical step to drop entirely the distinction between booster and main ring and think in terms of two identical rings. This in turn challenges us to explore the feasibility of colliding heavy ion beams.

Colliding Beam Performance

The design of a storage ring will be substantially more demanding than that of a straight forward synchrotron. Low β -insertions, possibly tuneable "in-flight" to avoid excessive quadrupole apertures at low energies, will be required and γ_{t} will either have to be changeable by $\sim \pm 1$ or moved above the operating range. Experimental insertions will require zero dispersion while others (for stacking) need non-zero dispersion. This should indicate a few complications just with regard to lattice design. It is mandatory that we explore carefully expected performance for the colliding beam mode. First, tolerable current levels will be established, then from this the corresponding luminosity.

Incoherent Tune Shifts - For a nearly round, nearly centered beam in a circular enclosure of diameter much larger than the beam the incoherent tune shift is dominated by the direct terms even at energies of 10 to 20 GeV/amu, and the limiting current (in particle amp) is given by the usual expression:

$$I = \frac{ec}{R} \cdot \frac{A}{q^2} \cdot \frac{\Delta v}{r_p} \cdot H_f \cdot \beta^2 \left(\frac{1}{\gamma^2} - \eta_e \right)^{-1} \cdot \epsilon_N \quad (1)$$

For coasting beams ($\beta_z = 1$), $\Delta v = 0.05$, $A = 200$, $q = 80$ and a normalized emittance $\epsilon_N = 3 \cdot 10^{-5}$ m, $I > 0.5$ particle A results for $\gamma \geq 7$ (Fig. 6). The neutralization will be kept low by clearing electrodes, a maximum value from considerations of the ion-electron instability has not yet been determined.

Longitudinal Stability

From the well known stability criterion¹⁵)

$$\left| \frac{\delta_{11}}{n} \right| \leq F \cdot \frac{A}{q^2} \cdot \frac{\beta^2 \gamma \epsilon_0}{e} \cdot \frac{|\eta|}{I} \cdot \left(\frac{\Delta p}{p} \right)^2 \quad (2)$$

the most stringent limitation is obtained if it is applied to a single, debunched pulse from the synchrotron. Assuming $2 \cdot 10^{11}$ particles ($q/A = 80/200$) a minimum tolerable $\frac{\Delta p}{p}$ is computed from which in turn, for a given stack momentum width a maximum number of stacked pulses and therefore a limit on obtainable circulating current is obtained. (Fig. 7).

Intra-Beam Scattering - This was explored using lattice functions from preliminary designs and the theory developed by A. Piwinsky^{16,17}). Growth and decay times of emittances are given by:

$$\tau_z^{-1} = A f(a, b, c)$$

$$\tau_x^{-1} = A f(a/b, 1/b, c/b) + (1-T)f(b/a, 1/a, c/a) \quad (3)$$

$$\tau_p^{-1} = 2A T f(b/a, 1/a, c/a)$$

We refer to the literature¹⁷) for the meaning of these quantities, suffice it to say that $f(1,1,c) = 0$, from which for $\beta_x = \beta_z$ an equilibrium condition with:

$$\epsilon_{z,N} = \epsilon_{x,N} = \epsilon_N; \delta_T = \frac{\pi \epsilon_N}{\beta_x} \cdot \frac{1}{\gamma} \cdot \frac{1}{\eta} \quad (4)$$

is predicted, realizable obviously only below transition ($\eta > 0$). From δ_T , the total stack momentum width from (4), again a maximum number of stacked pulses and a current limitation is obtained which, below transition, for our parameters is very close to the limits imposed by the $\Delta v = 0.05$ requirement (Fig. 8). Above transition no such equilibrium exists, for $\epsilon_N = 3 \cdot 10^{-5}$ m, $\delta_T = 2 \cdot 10^{-2}$, time constants $-\tau_z \sim \tau_x \sim \tau_p \sim 10^3$ s follow for 0.2 particle A circulating current. These values might be just slow enough for colliding beam operation. Furthermore a low noise (certainly possible with $q = 80$, $N \sim 5 \cdot 10^{12}$) stochastic cooling system with a bandwidth of 2-3 GHz should be able to provide cooling times of a few 10^4 s, capable of counteracting beam blow-up by intra-beam scattering.

Pressure Bump - Wall surfaces have been prepared to show a negative net ion induced desorption coefficient η ¹⁸) in which case beam pumping rather than a beam induced pressure rise occurs and no limiting current exists. Assuming $\eta \sim 3$, closely spaced pumps, compatible with the short magnets envisaged for this lattice, $\sigma_{80,200}(CO) = 80^2 \sigma_{1,1}(CO)$ a limiting current of 0.34 pA is obtained with a bore radius of 8 cm. Clearly the possibility of using a cold bore must also be explored and for purposes of estimating luminosity we assume $I = 0.2$ particle A for $A = 200$. A summary of these current limitations is given in Fig. 9.

Luminosity Estimates

Luminosity was estimated on the basis of 0.2 pA coasting beams for the heaviest ions. For head-on collisions ($\psi = 0$) the luminosity is:

$$L = \frac{2 I^2}{e^2 c \pi} \cdot \frac{d}{e \delta_{11}} \quad (5)$$

valid for $\beta_x, I = \beta_z, I = \beta_I$ and $d \leq 2 \beta_I$. For a given current and emittance then the only free parameter is β_I because d is constrained by the requirement that the beam-beam tune shift must not exceed a

certain limit. From:

$$\Delta v^{bb} \approx 8k^{bb} \cdot \frac{q^2}{A} \cdot \frac{I d}{p \epsilon}; k^{bb} \approx 2.386 \cdot 10^{-9} [A^{-1} \cdot \text{GeV}/c/\text{amu}] \quad (6)$$

we obtain $d \approx 1.25 \text{ m}$ independent of momentum p for $\epsilon_N = \epsilon_B = 3 \cdot 10^{-5} \text{ m}$ and $\Delta v^{bb} = 0.005$. With β_I as low as 0.5 m both luminosity and tune shift equations as given are still quite accurate and for $\beta_I = 1 \text{ m}$, $L > 10^{29} \text{ cm}^{-2} \text{ s}^{-1}$ seems achievable for the heaviest ion beams.

Such a short interaction length requires a bending magnet arrangement somewhat restricting free space immediately around the interaction point and $\psi \neq 0$ might be more desirable.

We have in this case:

$$L \approx \frac{2 I^2}{e^2 c \sqrt{\pi} \epsilon^{1/2} \beta_{z,1}^{1/2}} \cdot \frac{1}{\psi} \quad (7)$$

$$\Delta v^{bb} \approx 8 \sqrt{2\pi} k^{bb} \cdot \frac{q^2}{A} \cdot \frac{1}{\beta} \cdot \frac{I \beta_I^{1/2}}{\psi \epsilon^{1/2}}$$

For given I and ϵ, ψ and $\beta_{z,1}$ must now be adjusted to maximize L subject to $\Delta v \leq 0.005$. Again the validity of the simple tuneshift expression is restricted, breaking down for extremely small β_I and ψ (19,20). At $\beta_{z,1} = 1 \text{ m}$ and the values of ψ resulting from $\Delta v^{bb} = 0.005, 2.5 \text{ mrad}$ (at $20 \text{ GeV}/\text{amu}$) $\leq \psi \leq 6 \text{ mrad}$ (at $4 \text{ GeV}/\text{amu}$) it is however still quite accurate. The resulting luminosity is shown in Fig. 10.

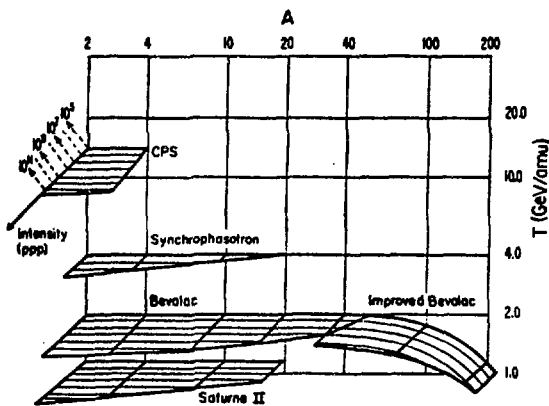
Conclusion

The first major new relativistic heavy ion facility may not look like what is described here but may well be a straightforward synchrotron with conventional magnets, approximately of the size of the CPS or AGS. We believe however to have demonstrated, at least in principle, the feasibility of a far advanced approach, posing many challenging design problems which should however not deter us if this should be the research tool needed for the exploration of relativistic heavy ion collision in the future.

References

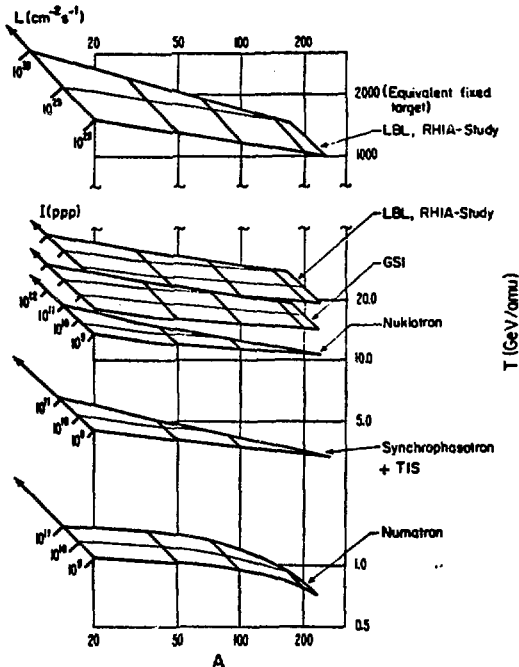
1. P. Asboe-Hansen, et al, IEEE, NS-24, No. 3, 1977, p1557-1560.
2. J. L. Laclare, GSI, -p-5-78, Vol. e, 1978, p 468-469.
3. H. A. Grunder, F. B. Selph, Proc. 1976 Proton Linear Accel. Conf., 1976, p 54-61.
4. J. Staples, this conference.
5. Conceptual Design Report "High Intensity Uranium Beams" from SuperHILAC and the Bevalac, Lawrence Berkeley Laboratory, June 1978.
6. Untersuchungen zu einen Schwerionen-Synchrotron, GSI, Dec. 1978.
7. Relativistic Heavy Ion Accelerators, H. A. Grunder, C. W. Leemann, F. B. Selph, LBL, p 321, Proc. of the X International Conference on High Energy Accelerators, Serpukhov, USSR, 1977.
8. H. A. Grunder, Ch. Leemann, F. Selph, GSI-p-5-78, p406-431, also LBL-7921, 1978.
9. Y. Hirao, GSI-p-5-78, p 461-467, 1978, also this conference.
10. B. Franzke et al, GSI-J-1-78, p 157-158, 1978
11. C. V. Pagan, IEEE, NS-24, No. 3, 1977, p 130-139
12. I.A. Snukeilo, Proc. Xth Int. Conf. High Energy Accel., vol. 1 p 339, 1977.
13. W. Gilbert, priv. communication

14. B. Franzke et al., GSI-PB-4-75, B1, 1975.
15. A. Hofmann, CERN 77-13, 139, 1977.
16. A. Piwinsky, Proc. IXth Int. Conf. High Energy Acce., 405, 1974.
17. H. Hahn et al, Rev. Mod. Phys., Vol 49, No. 3, 625-680, 1977
18. E. Fischer, IEEE, NS-24, No. 3, 1227-2332
19. G. Guignard, CERN 77-10, 1977
20. E. Keil, CERN 77-13, p 314-340, 1977



XBL 793-8712

Fig. 1 Present Facilities, Beam Performance as obtained or predicted for near future



XBL 793-834

Fig. 2 Approximate performance goals of presently investigated concepts of new facilities

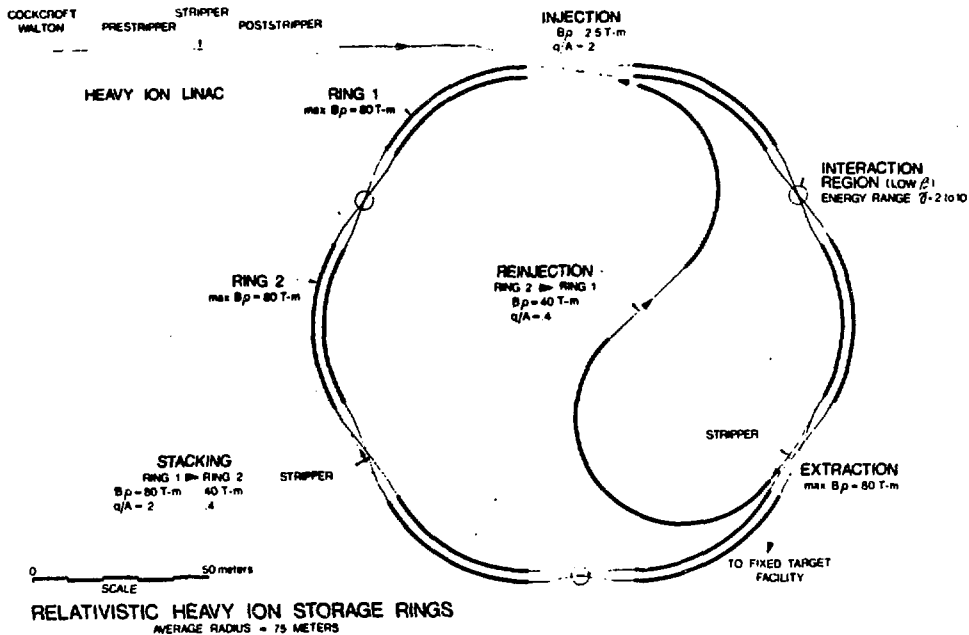


Fig. 3 Accelerator/Storage ring concept from preliminary LBL-studies. B_0 assumed in this paper is 175 Tm, $B_{max} = 5T$, $\bar{B} = IT$

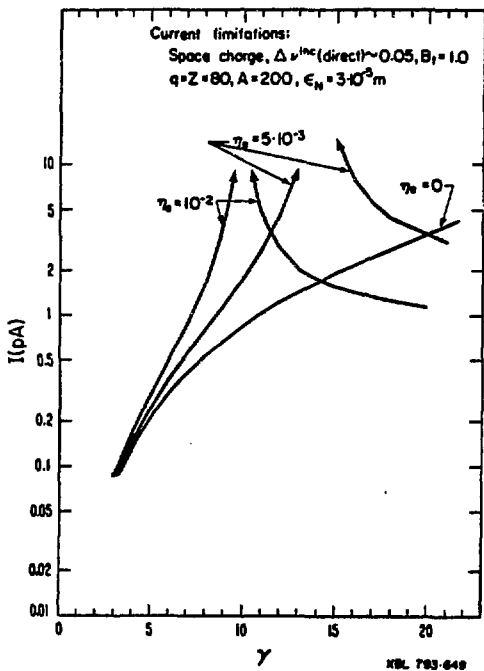


Fig. 6 Space charge limited currents for parameters indicated in figure.

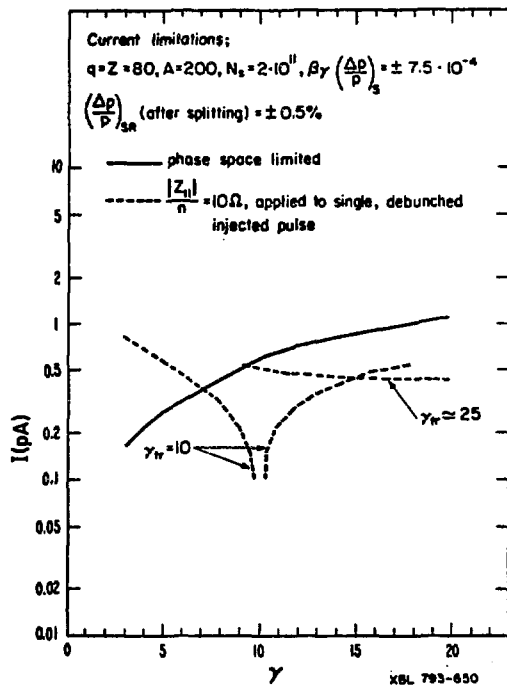


Fig. 7 Current limitations from longitudinal stability considerations (dashed lines), from linac momentum spread (solid lines).

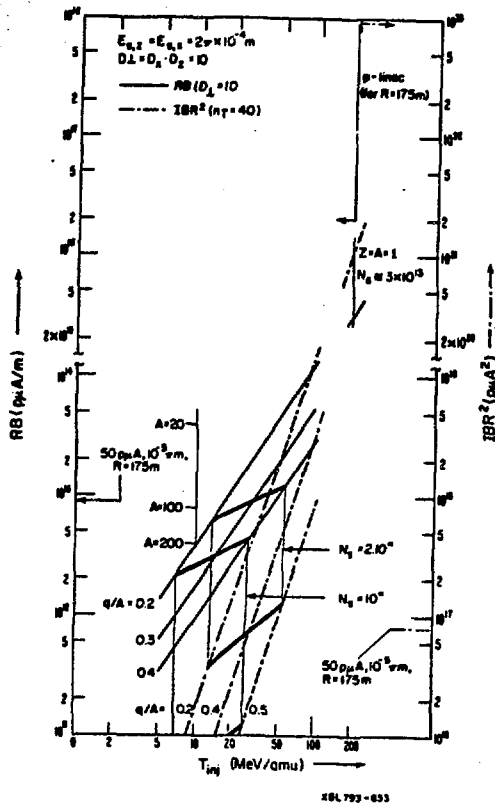


Fig. 4 Linac brightness B (solid lines), current-brightness product IB (dashed lines), multiplied by R , R^2 respectively, as required to reach space charge limit N_B in synchrotron for $A = 200$. Assumed is total transverse dilution $D_1 = D_x \cdot D_z = 10$, number of injected turns = 40, horizontal and vertical acceptance = $2\pi \cdot 10^{-6}$ m. Heavy solid lines correspond to $N_B = 2 \cdot 10^{11}$ and 10^{11} respectively.

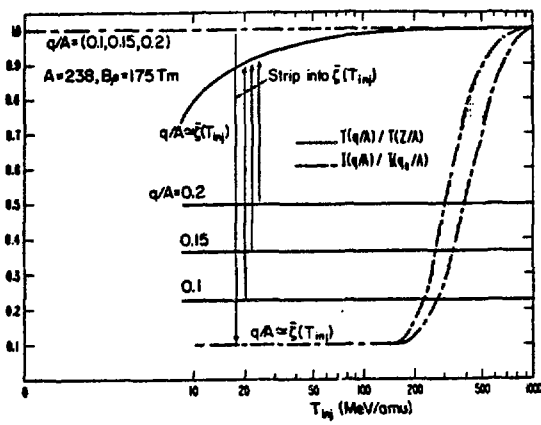


Fig. 5 Solid lines indicate kinetic energy obtainable with given q/A , with and without stripping at linac exit normalized to $T(Z/A)$. Dashed lines indicate corresponding intensity, normalized to intensity obtained without stripping.

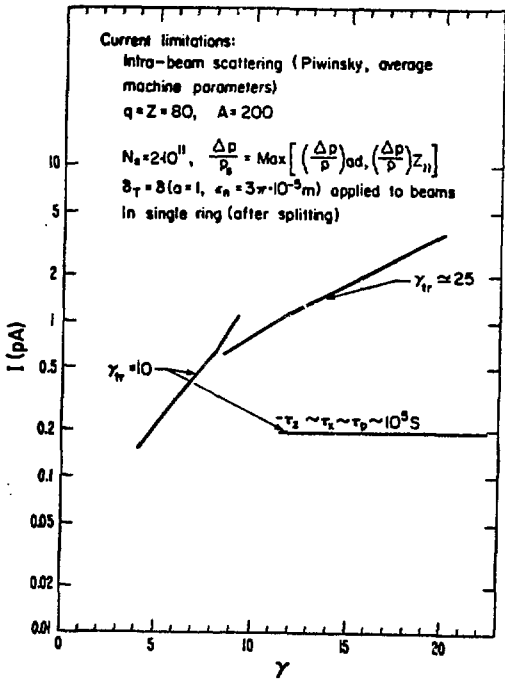
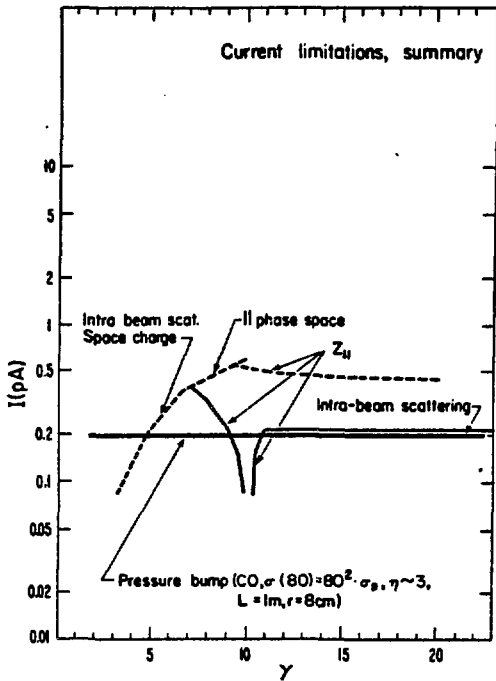
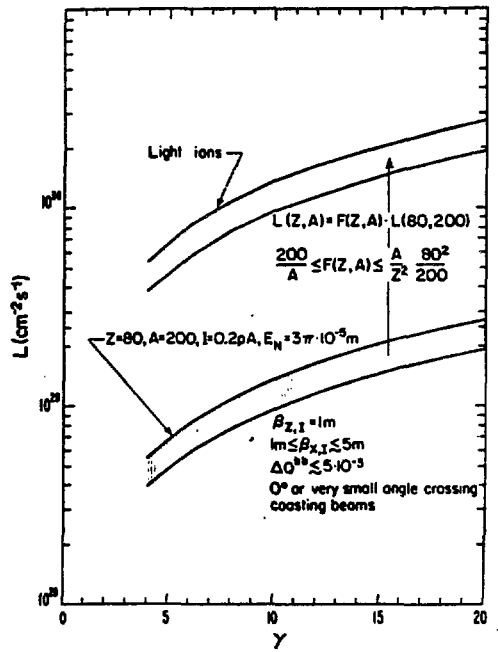


Fig. 8 Current limitations from intra-beam scattering.



XBL 793-652

Fig. 9 Summary of currents limitations, including estimate of limitation imposed by pressure-bump phenomenon.



XBL 792-647

Fig. 10 Luminosity estimates for parameters indicated in figure

STABILITY OF INTENSE TRANSPORTED BEAMS*

L. J. Laslett and Lloyd Smith**

Summary

At the previous National Accelerator Conference, the transport of intense ion beams, with particular reference to Heavy Ion Fusion, was analyzed by finding matched solutions of the coupled envelope equations.¹⁾ This work established relations between lattice structure, beam dimensions and space-charge tune depression as a function of intensity. In this paper we report on an investigation of the stability of the K-V distribution in transport by a periodic quadrupole system, a generalization of Gluckstern's analysis for a continuous solenoid.²⁾ The results are presented and compared with simulation computations for a particular case; the results provide a prediction of maximum transportable current without degradation of emittance due to instability.

Method³⁾

The K-V distribution is unique in that it permits specification of a stationary state in the presence of variable linear external forces plus space charge forces. Since the motion of individual ions is governed by linear forces, a perturbed solution of Vlasov's equation can be usefully written as an integral of the perturbing forces along the unperturbed trajectories. The forces, in turn, are determined by Poisson's equation in the two transverse dimensions; integration of the perturbed distribution function over the transverse momentum variables then leads to an integro-differential equation for the perturbed potential of the form:

$$\frac{1}{a^2} \frac{\partial^2 V}{\partial x^2} + \frac{1}{b^2} \frac{\partial^2 V}{\partial y^2} = - \frac{Q}{\pi e a b} \int_{-\infty}^s ds' \left[\frac{\partial}{\partial \psi_x} r + \frac{\partial}{\partial \psi_y} r \right] \int_0^{2\pi} d\theta V(x', y', s') \quad (1)$$

where $x' \equiv x(s') = x(s) \cos [\psi_x(s') - \psi_x(s)]$

$$+ p(s) \cos \theta \sin [\psi_x(s') - \psi_x(s)]$$

$$y' \equiv y(s') = y(s) \cos [\psi_y(s') - \psi_y(s)]$$

$$+ p(s) \sin \theta \sin [\psi_y(s') - \psi_y(s)]$$

$$\psi_{x,y}(s) = \int \frac{ds}{\beta_{x,y}}$$

$$Q = \frac{4Nq}{AB^2 Y^3} r_p, \text{ where } N = \text{number of particles per unit length of beam}$$

πe = emittance (assumed equal in both planes)

a, b = half width of the beam in x and y , respectively.

$\beta_{x,y}$ and a, b are periodic functions of s , determined as in reference (1).

*This work was supported by the Office of Inertial Fusion Division of the U.S. Department of Energy under contract No. W-7405-RNG-48.

**Lawrence Berkeley Laboratory, Berkeley, CA 94720

In spite of the formidable appearance of eq'n (1), a brief inspection shows that the solutions for $V(x, y, s)$ are mixed finite polynomials in x and y with coefficients that are functions of s . Eq'n (1) then reduces to a set of linear differential equations involving the coefficients. Finally, a numerical integration of these equations through one period using the appropriate $a(s)$ and $b(s)$ leads to a matrix, the eigen-values of which determine whether the motion is stable or unstable in the presence of that form of perturbation.

Results

We use a terminology in which an n^{th} order perturbation is one in which n is the highest power appearing in the perturbed potential; it is further called even or odd according to whether even or odd powers of y occur. Thus, for example, $V = Ax^4 + Bx^2y^2 + Cy^4$ is "fourth order even" and $V = Ax^2y + By^3$ is "third order odd". In practice, the number of equations for the coefficients increases so rapidly with order that we have not gone beyond sixth order. A finer grained structure to the perturbation is in fact not very interesting in view of the doubtful relation of the K-V distribution to a real beam.

The general character of the results is that instability occurs for all modes in finite ranges of intensity such that the frequencies of the modes pass through a rational relation to the Fourier components of the β -functions. In addition, for the even order modes a threshold is reached above which the motion is unstable for all higher intensities. For reasons not fully understood, these thresholds occur at precisely the same tune depression as for the continuous solenoid and the growth rates as functions of further tune depressions are precisely the same. Fig's 1 and 2 show the unstable regions for fourth and sixth order even perturbations for a FODO lattice with various zero-intensity phase advances per period.

The second order even perturbation ($V = Ax^2 + By^2$) corresponds to integrating the envelope equations with a slight initial mis-match. This mode is unstable at an intensity which depresses the phase advance per cell to 90° if the zero intensity phase advance per cell is greater than 90° . On the basis of this result we feel that a transport channel for high intensity beams should be designed for less than 90° at zero intensity.

Comparison with Simulation Computations

In parallel with the analytic work, extensive simulation computations have been carried out by Haber.⁴⁾ We find qualitative agreement for the onset of the extended region of instability but, since many modes are unstable in this region, a quantitative comparison is not possible. However, in a different parameter range, Haber found an instability which we were able to identify as an isolated third order structure resonance. From the perturbed distribution function for the mode, expressions for the growth of various moments of the distribution and the distortion of the phase space boundaries were derived and compared, period by period, with the simulation results. Surprisingly good agreement was found for the growth rate, the relative magnitudes of the moments and the boundary distortions, the only empirical parameters being the effective initial amplitudes of the odd and even modes. Figure 3 illustrates the development of this instability as the intensity is increased, the larger of the two

180-deg. modes being identifiable with the instability observed by Haber (with $\sigma \cong 46$ deg.) Figure 4 shows a typical comparison of moments and Figure 5 the distortion of the emittance ellipse. This comparison provides a check on both the theory and the simulation work, and lends credence to the simulation of distributions which are not accessible to theory.

Conclusions

Because of the singular nature of the K-V distribution, it is somewhat more susceptible to instability than a more realistic distribution. Therefore, avoidance of these instabilities should provide a conservative criterion for design of a transport channel. In this spirit, the zero-intensity phase advance should be less than 60° in order to avoid the envelope and third order instabilities and then one should limit the current to a tune depression of a factor of 2.5 (e.g., 60° to 24°), at which intensity the extended unstable range begins to appear. In the notation of eq'n (3) of reference (1), the corresponding figure of merit, $Q'/u_m^{2/3}$, is then only a function of the fraction of the channel occupied by quadrupoles, as shown in Table 1.

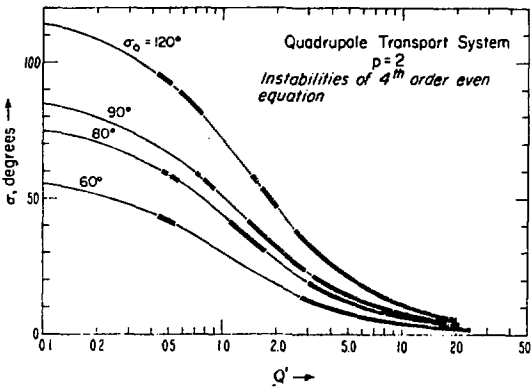


Fig. 1. Regions of fourth-order even instability (heavy lines) for a symmetric FODO quadrupole lattice with a magnet occupancy factor $n = 1/2$.

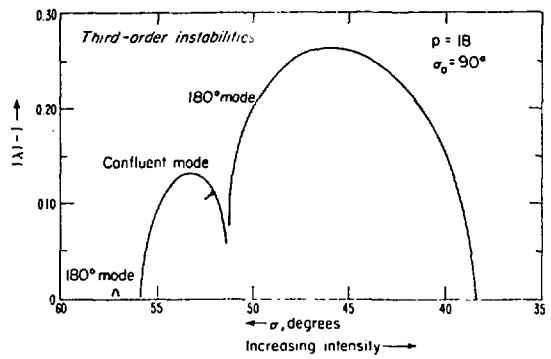


Fig. 3. Instability regions for the third-order mode. The curves represent the growth per period calculated for $n = 1/10$, but are very insensitive to n when plotted vs. σ .

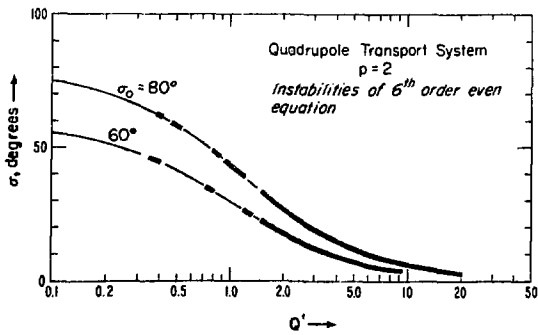


Fig. 2. Regions of sixth-order even instability for $n = 1/2$.

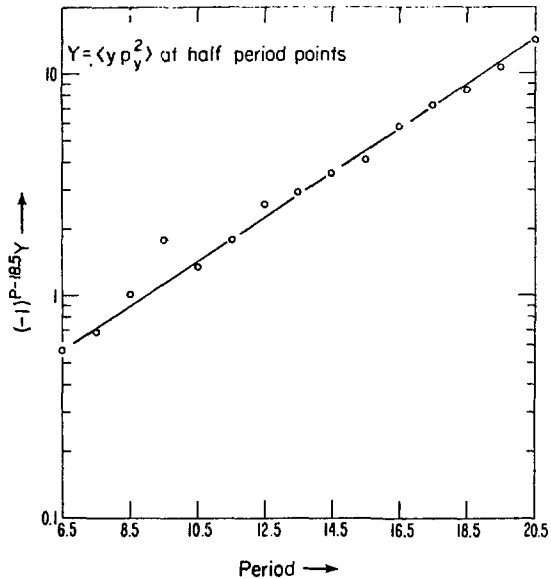


Fig. 4. Illustration of exponential growth of $\langle y p_y^2 \rangle$ found in simulation computations and attributed to the third-order mode instability.

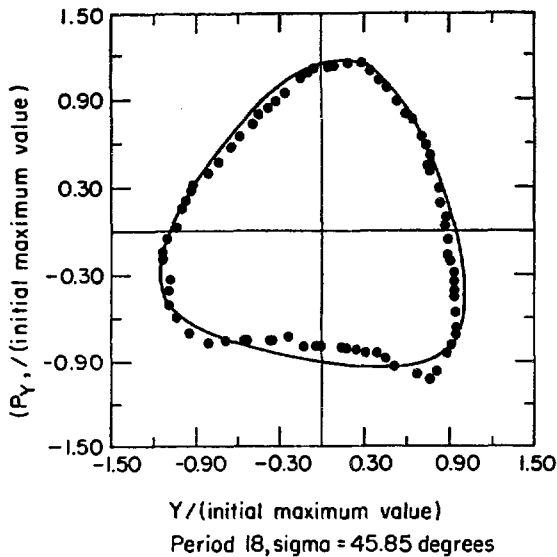


Fig. 5. Boundary of computed distribution in a y, p_y projection.

Acknowledgements

We have benefited greatly from numerous discussions with many of our colleagues during this work and it is a particular pleasure to express our thanks explicitly to Victor O. Brady, Swapan Chattopadhyay, Irving Haber, and Ingo Hofmann for their assistance.

Table I.

Figures of Merit for $\sigma_0 = 60$ Deg. & $\sigma = 24$ Deg.

η^*	$Q' = Q/(e\sqrt{K})$	$[FM] = Q'/u_m^{2/3}$
1	1.6581	0.764
2/3	1.5392	0.688
1/2	1.3959	0.601
1/3	1.1851	0.481
1/4	1.0445	0.405
1/5	0.9436	0.354
1/6	0.8669	0.315
1/8	0.7567	0.263
1/10	0.6799	0.228

* η denotes the magnet occupancy factor.

References

1. G. Lambertson, L.J. Laslett, and L. Smith, IEEE Trans., Nucl. Sci., NS-24, p. 993, June 1977.
2. R.L. Gluckstern, Proc. 1970 Proton Linac Conference (NAL), p. 811.
3. The theory and results are described in detail in LBL HI-FAM notes 13, 14, 15, 43 and 44.
4. See I. Haber, report in proceedings of this conference.

APPENDIX H

LONGITUDINAL MOTION IN HIGH CURRENT ION BEAMS - A SELF-CONSISTENT PHASE SPACE DISTRIBUTION WITH AN ENVELOPE EQUATION*

David Neuffer**

Summary

Many applications of particle acceleration, such as heavy ion fusion, require longitudinal bunching of a high intensity particle beam to extremely high particle currents with correspondingly high space charge forces. This requires a precise analysis of longitudinal motion including stability analysis. Previous

papers^{1,2)} have treated the longitudinal space charge force as strictly linear, and have not been self-consistent; that is, they have not displayed a phase space distribution consistent with this linear force so that the transport of the phase space distribution could be followed, and departures from linearity could be analyzed. This is unlike the situation for transverse phase space where the Kapchinskij-Vladimirskij (K-V)³⁾ distribution can be used as the basis of an analysis of transverse motion. In this paper we derive a self-consistent particle distribution in longitudinal phase space which is a solution of the Vlasov equation and derive an envelope equation for this solution. The solution is developed in Section II from a stationary solution of the Vlasov equation derived in Section I.

I. An Example of a Stationary Distribution for Longitudinal Transport

In these calculations we assume the longitudinal and transverse motion of particles in the beam bunch are completely decoupled with the beam length much greater than the beam radius. We choose the longitudinal distance from the center of the bunch z and the position of the center of the bunch s as the dependent and independent variables.

The ions in the bunch experience a space charge force given by ⁴⁾

$$F_z = -\frac{q}{\gamma} \frac{q^2 e^2}{2} \frac{d\lambda}{dz} \quad (1)$$

where q is the ion charge state, λ is the number of ions per unit length, and g is a geometrical factor of order unity.

We simplify the discussion by assuming the center of the bunch is not accelerating but moves with constant speed Bc , and rewrite (1) (non-relativistically) as

$$\frac{d^2 z}{ds^2} = z'' = -\frac{q^2 e^2}{\beta^2 c^2 M} \frac{d\lambda}{dz} = -A \frac{d\lambda}{dz} \quad (2)$$

where M is the ion mass and the ' symbol denotes differentiation with respect to s . This is a debunching force and tends to extend the bunch. We add a linear bunching force F_B by applying a linearly ramped external electric field $E_z = E'z$ so that $F_B = qeE'z$. We define a bunching parameter K by the equation $F_B = -MK\beta^2 c^2 z$ and obtain the equation of motion

$$z'' = -A \frac{d\lambda}{dz} - Kz \quad (3)$$

and we associate this equation of motion (3) with a massless Hamiltonian:

$$H \equiv \frac{z'^2}{2} + A\lambda + \frac{Kz^2}{2} + H_0 \quad (4)$$

The Vlasov equation for the z - z' phase space distribution $f(z, z', s)$ from this Hamiltonian is:

$$\frac{\partial f}{\partial s} + z' \frac{\partial f}{\partial z} + (-A \frac{\partial \lambda}{\partial z} - Kz) \frac{\partial f}{\partial z'} = 0 \quad (5)$$

If we choose f such that $f = f(H)$ then the Vlasov equation requires that $\frac{\partial f}{\partial s} = 0$ and we have a stationary distribution. We must also choose an f that is self-consistent; that is

$$\int f(z', z, s) dz' = \lambda(z, s) \quad (6)$$

As a simplest solution we desire $\lambda(z)$ to be parabolic:

$$\lambda = \frac{3}{4} \frac{N}{z_m} \left(1 - \frac{z^2}{z_m^2}\right) \equiv \lambda_0 \left(1 - \frac{z^2}{z_m^2}\right) \quad |z| < z_m$$

$$\lambda = 0 \quad |z| > z_m \quad (7)$$

where N is the total number of ions in the bunch and $2z_m$ is the length of the bunch. This gives a linear

space charge force of $\frac{2A\lambda_0 z}{z_m}$. We choose $H_0 = -A\lambda_0$ and

define a reduced bunching parameter K^1 by

$$H = \frac{z'^2}{2} + \frac{1}{2} \left(K - \frac{2A\lambda_0}{z_m}\right) z^2 = \frac{z'^2}{2} + \frac{K^1}{2} z^2$$

with $K^1 \equiv K - \frac{2A\lambda_0}{z_m}$ (8)

For an ansatz we choose:

$$f(H) = C \sqrt{2(H_{\max} - H)} = C \sqrt{2H_{\max} - K^1 z^2 - z'^2}$$

for $0 < H < H_{\max}$

$$f(H) = 0 \text{ for } H > H_{\max} \quad (9)$$

Writing $2H_{\max} \equiv K^1 z_m^2$, we check that this distribution satisfies the condition (6), that is

$$\int_{z'_{\min}}^{z'_{\max}} C \sqrt{K^1 z_m^2 - K^1 z^2 - z'^2} dz' = \lambda(z) \quad (10)$$

The limits of integration can be found from (9):

$$z'_{\max} = -z'_{\min} = \sqrt{K^1 (z_m^2 - z^2)}$$

We integrate and find:

$$\lambda(z) = \frac{CmK^1 z_m^2}{2} \left(1 - \frac{z^2}{z_m^2}\right) \quad (11)$$

*This work was supported by the Office of Inertial Fusion Division of the U.S. Department of Energy under contract No. W-7405-ENG-48.

**Lawrence Berkeley Laboratory, Berkeley, CA 94720

This agrees with (7) if we choose the value of C as

$$C = \frac{2\lambda_0}{\pi k z_m^2} = \frac{2\lambda_0}{\pi(Kz_m^2 - 2A\lambda_0)} \quad (12)$$

The three interdependent parameters λ_0 , z_m , K define a consistent solution. Two of the parameters are set by internal properties of the beam bunch: its longitudinal emittance ϵ_L and the total number of ions

N. We display the relationships:

$$N = \frac{4}{3} \lambda_0 z_m \quad (13)$$

and

$$\begin{aligned} \epsilon_L = z_{\max} \cdot z'_{\max} (z=0) &= (K^2)^{1/2} z_m^2 \\ &= \left(K - \frac{2A\lambda_0}{z_m^2}\right)^{1/2} z_m^2 \end{aligned} \quad (14)$$

The third parameter, which we associate with the external field k , may be chosen arbitrarily, but K must be positive. Equations (13, 14) can be combined to give

$$\epsilon_L^2 + \frac{3}{2} ANz_m - Kz_m^4 = 0 \quad (14A)$$

which can then be solved for z_m .

Consideration of the three dimensional problem with the requirement of transverse (x-y) stability may set an upper limit λ_{\max} on λ_0 , the maximum ion density.

This would set a lower limit on z_m ($z_m > \frac{3}{4} \frac{N}{\lambda_{\max}}$), which

would mean an upper limit on K obtainable from the solution of equation (14A) with the limiting value of z_m .

II. Envelope Equation for Longitudinal Motion

The existence of a stationary solution of the longitudinal transport problem of form (9) suggests that a similar solution $f(z, z', s)$ that is not stationary can be found. As our ansatz we choose

$$f(z, z', s) = D \sqrt{1 - \frac{z^2}{z_0^2} - \frac{(z' - Bz)^2}{a_s^2}} \quad (15)$$

in the region $\frac{z^2}{z_0^2} + \frac{(z' - Bz)^2}{a_s^2} < 1$

($f(z, z', s) = 0$ otherwise),

where the parameters D , z_0 , a_s , B are functions of s whose behavior is determined by requiring that f satisfy the Vlasov equation.

We find:

$$\begin{aligned} \lambda &= \int_{z'_{\min}}^{z'_{\max}} D \sqrt{1 - \frac{z^2}{z_0^2} - \frac{(z' - Bz)^2}{a_s^2}} dz' \\ &= \frac{\pi}{2} a_s D \left(1 - \frac{z^2}{z_0^2}\right) \equiv \lambda_0 \left(1 - \frac{z^2}{z_0^2}\right) \end{aligned} \quad (16)$$

We include an external linear focussing field of arbitrary value Kz , so that

$$z'' = -A \frac{d\lambda}{dz} - Kz = \left(-\frac{2A\lambda_0}{z_0^2} - K\right) z \quad (17)$$

From the Vlasov equation:

$$\frac{\partial f}{\partial s} + z' \frac{\partial f}{\partial z} + z'' \frac{\partial f}{\partial z'} = 0 \quad (18)$$

We find $\frac{\partial D}{\partial s} = 0$ (18A)

$$a_s = \frac{\epsilon_L}{z_0}, \text{ where } \epsilon_L \text{ is some constant} \quad (18B)$$

$$B = \frac{dz_0}{ds} / z_0 = \frac{z'_0}{z_0} \quad (18C)$$

and we find an envelope equation for z_0

$$\frac{d^2 z_0}{ds^2} = \frac{\epsilon_L^2}{z_0^3} + \frac{2A\lambda_0}{z_0} - Kz_0 \quad (18D)$$

Identifying λ_0 as $\frac{3}{4} \frac{N}{z_0}$ from (7)

and noting $D = \frac{3N}{2\pi\epsilon_L}$ from (16),

we obtain a self-consistent solution to the Vlasov equation:

$$f(z, z', s) = \frac{3N}{2\pi\epsilon_L} \sqrt{1 - \frac{z^2}{z_0^2} - \frac{z_0^2}{\epsilon_L^2} \left(z' - \frac{z'_0}{z_0} z\right)^2} \quad (19)$$

wherever the argument of the square root is real ($f = 0$ otherwise), and where z_0 is a solution of the envelope equation:

$$\frac{d^2 z_0}{ds^2} = \frac{\epsilon_L^2}{z_0^3} + \frac{3}{2} \frac{AN}{z_0^2} - Kz_0 \quad (20)$$

The initial conditions $z_0(s=0)$ and $z'_0(s=0)$ may be chosen arbitrarily and K may be an arbitrary function of s .

This equation is the same envelope equation derived earlier from a non-self-consistent perspective¹⁾ and is similar to the K-V equations. The quantity $\frac{z^2}{z_0^2} + \frac{z_0^2}{\epsilon_L^2} \left(z' - \frac{z'_0}{z_0} z\right)^2$ is an invariant similar to the transverse Courant-Snyder invariant.⁵⁾ The stationary solution derived in the previous section is simply the special solution of equations (19, 20) where ϵ_L , z_0 ,

K and N are chosen in a combination such that $\frac{d^2 z_0}{ds^2}$ is set equal to zero, and also z'_0 is initially zero.

The similarity between the longitudinal envelope equation (20), and the K-V equations suggests that an analysis of stability of the longitudinal envelope similar to the earlier analysis of the transverse K-V

envelope⁶⁾ would be of similar value in identifying instabilities. Results of this analysis will be presented in future papers.

We thank L. Smith and D. Keefe for helpful conversations.

References

1. L. Smith, "ERDA Summer Study for Heavy Ions for Inertial Fusion", LBL-5543 (1976), p. 77.
2. D. Judd, "Proceedings of the Heavy Ion Fusion Workshop", BNL-50769 (1977), p.34.
3. I.M. Kapchinskij and V.V. Vladimirskej, Proc. Int. Conf. on High Energy Accelerators, CERN (1959), p. 274.
4. A. Hofmann, "Theoretical Aspects of the Behavior of Beams in Accelerators and Storage Rings", CERN 77-13 (1977), p. 139.
5. E. Courant and H. Snyder, Annals of Physics 3, p. 1 (1958).
6. I. Smith, S. Chattopadhyay, I. Hofmann, and L.J. Laslett, "Stability of the K-V Distribution in Long Periodic Systems", HI-FAN-13, HI-FAN-14, HI-FAN-15, Lawrence Berkeley Laboratory (1977).